



# BATHYMETRIC AND TOPOGRAPHIC SURVEYING OF FLOOD-PRONE RIVERS IN DAR ES SALAAM

Comparative Case of UAV Photogrammetry and UAV LiDAR for  
Generation of Digital Terrain Models for Flood Modelling Purposes  
*Msimbazi River, Dar es Salaam*

August 7<sup>th</sup> 2019

For  
The World Bank

Client:



Financier:



Contractor:





# BATHYMETRIC AND TOPOGRAPHIC SURVEYING OF FLOOD-PRONE RIVERS IN DAR ES SALAAM

Comparative Case of UAV Photogrammetry and UAV LiDAR for  
Generation of Digital Terrain Models for Flood Modelling Purposes  
*Msimbazi River, Dar es Salaam*

**Document** UAV DTM Comparison Report  
**Status** Final  
**Code** B1809-07-R001  
**Revision** 2.0  
**Date** August 7<sup>th</sup> 2019

Rev.	Description	Prepared	Approved	Date
1.0	Draft	Roeland de Zeeuw <sup>1</sup> & Bas van de Sande <sup>2</sup>	D. Heijboer <sup>2</sup>	May 15, 2019
2.0	Final	Roeland de Zeeuw <sup>1</sup> & Bas van de Sande <sup>2</sup>	D. Heijboer <sup>2</sup>	August 7, 2019

**<sup>1</sup>Shore Monitoring and Research BV**  
2<sup>e</sup> Zeesluisdarsweg 8  
2583 DW Den Haag  
Netherlands  
Telephone: +31 6 8128 0230  
E-Mail: [info@shoremonitoring.nl](mailto:info@shoremonitoring.nl)  
Web: [www.shoremonitoring.nl](http://www.shoremonitoring.nl)  
CoC/Kvk: 63003112

**<sup>2</sup>CDR International BV**  
Koningin Wilhelminalaan 43  
3818HN Amersfoort  
Netherlands  
Telephone: +31 8 5301 0885  
E-Mail: [info@cdr-international.nl](mailto:info@cdr-international.nl)  
Web: [www.cdr-international.nl](http://www.cdr-international.nl)  
CoC/Kvk: 56270127

# TABLE OF CONTENTS

	Page
<b>1. EXECUTIVE SUMMARY.....</b>	<b>1</b>
<b>2. BACKGROUND.....</b>	<b>3</b>
<b>3. INTEGRAL SURVEY CAMPAIGN .....</b>	<b>5</b>
3.1 STUDY AREA.....	5
3.2 SURVEY COMPONENTS.....	6
<b>4. COMPARISON OF UAV LIDAR AND UAV PHOTOGRAMMETRY FOR DTM GENERATION .....</b>	<b>9</b>
4.1 PRINCIPLES OF MEASUREMENT TECHNIQUES .....	9
4.1.1 <i>Photogrammetry</i> .....	9
4.1.2 <i>LiDAR</i> .....	10
4.2 ACQUISITION.....	11
4.2.1 <i>Photogrammetry</i> .....	11
4.2.2 <i>LiDAR</i> .....	11
4.3 (POST)-PROCESSING TO DTM .....	12
4.3.1 <i>Photogrammetry</i> .....	12
4.3.2 <i>LiDAR</i> .....	13
4.4 DATA COMPARISON METHODOLOGY .....	14
4.4.1 <i>Introduction</i> .....	14
4.4.2 <i>Selection of typical terrain types</i> .....	15
4.4.3 <i>Performance assessment</i> .....	25
4.4.4 <i>Point cloud statistics</i> .....	25
4.4.5 <i>Land use on a basin scale level</i> .....	25
4.4.6 <i>Validation with GNSS data for typical terrain types</i> .....	26
<b>5. RESULTS .....</b>	<b>27</b>
5.1 PERFORMANCE TO MEASURE GROUND LEVEL .....	27
5.2 RESULTS OF STATISTICAL ANALYSIS .....	40
5.3 RESULTING UAV PHOTOGRAMMETRY AND LIDAR DTMS .....	44
5.4 CORRELATION WITH LAND USE MSIMBAZI BASIN .....	47
5.5 VALIDATION RESULTS GNSS.....	48
5.6 MAIN OBSERVATIONS .....	49
<b>6. IMPACT OF DTMS ON FLOOD MODELLING RESULTS .....</b>	<b>50</b>
6.1 COMPARISON OF UAV LIDAR DTM 2019 WITH DTM 2016 .....	50
6.2 HYDROLOGICAL AND HYDRODYNAMIC FLOOD MODEL USED.....	51
6.3 FLOOD MODELLING RESULTS.....	52
6.4 INTERPRETATION OF THE RESULTS .....	56
<b>7. CONCLUSIONS AND RECOMMENDATIONS .....</b>	<b>58</b>
7.1 CONCLUSIONS .....	58
7.2 RECOMMENDATIONS .....	60
<b>8. REFERENCES .....</b>	<b>62</b>

## LIST OF FIGURES

Figure 2-1: Spatial context of the Detailed Plan area of the MSDMF, which is the Study area for this Project.....	3
Figure 3-1: Study area.....	5
Figure 3-2: Setting out Ground Control Points and Benchmarks.....	6
Figure 3-3: Two left images showing the SBES bathymetric survey and the image right showing the RTK-GNSS survey by foot .....	7
Figure 3-4: Equipment configuration for both UAV LiDAR and UAV Photogrammetry.....	7
Figure 3-5: Location of installed water level logger underneath Selander Bridge .....	7
Figure 4-1: Overlapping aerial images taken from different positions and angles form the .....	9
Figure 4-2: Main equipment components for UAV LiDAR to enable direct measurements .....	10
Figure 4-3: Location of assessment areas (red) on background of orthophoto and OSM .....	15
Figure 4-4: Separated dense bushes with low vegetation, white polygon indicates assessment area. ....	16
Figure 4-5: Crop, trees and bare ground, white polygon indicates assessment area. ....	17
Figure 4-6: Dense medium tall vegetation, white polygon indicates assessment area. ....	17
Figure 4-7: Single bush and manmade shelter with bare ground, white polygon indicates assessment area. ....	18
Figure 4-8: Jangwani playing grounds, white polygon indicates assessment area.....	18
Figure 4-9: Bush and short grass with bare ground, white polygon indicates assessment area.....	19
Figure 4-10: Mangroves with dense canopy, white polygon indicates assessment area.....	19
Figure 4-11: Mangroves with less dense canopies, white polygon indicates assessment area. ....	20
Figure 4-12: Flattened reed, white polygon indicates assessment area. ....	20
Figure 4-13: Dense silver green vegetation, white polygon indicates assessment area. ....	21
Figure 4-14: Single tree, bush and silvery green vegetation.....	21
Figure 4-15: Trees dense.....	22
Figure 4-16: Variety of vegetation just south of Hanna Nassif.....	22
Figure 4-17: Long reed, not so dense .....	23
Figure 4-18: Bus depot.....	23
Figure 4-19: Morogoro Road.....	24
Figure 4-20: Typical urbanization, prone to flooding. ....	24
Figure 4-21: Validation points per class are indicated for bare ground, short grass, long grass and long reed. ....	26
Figure 5-1: Top view of the RGB coloured point cloud of the dense tree canopy area. Scale bar in meters.....	27
Figure 5-2: Side view of the RGB coloured point cloud of the dense tree canopy area. Ground points of LiDAR (brown) and photogrammetry (white) point clouds. Scale bar in meters. ....	28
Figure 5-3: Spatial distribution of the LiDAR (brown) and photogrammetry (white) ground points. Scale in meters. ....	28
Figure 5-4: Oblique view of the RGB coloured point cloud of the dense tree canopy area. Ground points of LiDAR (brown) and photogrammetry (white) point clouds. Scale bar in meters. ....	29
Figure 5-5: Side view of the RGB coloured point cloud of the mangroves area. Ground points of LiDAR (brown) and photogrammetry (white) point clouds. Scale bar in meters.....	29
Figure 5-6: Spatial distribution of the LiDAR (brown) and photogrammetry (white) ground points. Scale in meters.....	30
Figure 5-7: Top view of the RGB coloured point cloud of the less dense mangroves with bare ground visible. Ground points of LiDAR (brown) and photogrammetry (white) point clouds. Scale bar in meters. ....	30
Figure 5-8: Spatial distribution of the LiDAR (brown) and photogrammetry (white) ground points. Scale in meters. ....	31

Figure 5-9: Side view of the ground points of LiDAR (brown) and photogrammetry (white) point clouds. Scale bar in meters..... 31

Figure 5-10: Area type 10. Top view of the RGB coloured point cloud. Scale bar in meters..... 32

Figure 5-11: Oblique view of the RGB coloured point cloud of the dense tree canopy area. Ground points of LiDAR (brown) and photogrammetry (white) point clouds. Scale bar in meters. .... 32

Figure 5-12: Side view of the RGB coloured point cloud of the dense tree canopy area. Ground points of LiDAR (brown) and photogrammetry (white) point clouds. Scale bar in meters. .... 33

Figure 5-13: Top view of spatial distribution of the LiDAR ground points. Scale in meters. .... 33

Figure 5-14: Top view of RGB coloured area (left) and spatial distribution (right). Ground points of LiDAR (brown) and photogrammetry (white) point clouds. Scale bar in meters. .... 34

Figure 5-15: Top view of RGB coloured area (top), spatial distribution (middle) of and correctness (bottom) of ground points of LiDAR (brown) and photogrammetry (white) point clouds. Scale bar in meters. .... 35

Figure 5-16: Oblique view of RGB coloured area (top), spatial distribution (middle) of and side view of correctness (bottom) of ground points of LiDAR (brown) and photogrammetry (white) point clouds. Scale bar in meters..... 36

Figure 5-17: Top view of RGB coloured area (top). Oblique view of RGB coloured area and ground points of LiDAR (brown) and photogrammetry (white) point clouds. Scale bar in meters. .... 37

Figure 5-18: Top view of spatial distribution of LiDAR ground points (top) and side view of RGB coloured area and ground points of LiDAR (brown) and photogrammetry (white) point clouds. Scale bar in meters..... 38

Figure 5-19: Oblique view of RGB coloured area (top) and spatial distribution of LiDAR ground points (brown) photogrammetry (white) point clouds (bottom). Scale bar in meters. .... 39

Figure 5-20: 0.25 m resolution DTMs of Lidar (top), photogrammetry (middle) and elevation difference (bottom). Note scale of elevation differences in the figure in (m)..... 45

Figure 5-21: 2.0 m resolution DTMs of Lidar (top), photogrammetry (middle) and elevation difference (bottom). Note scale of elevation differences in the figure in (m)..... 46

Figure 5-22: Aggregated vegetated areas (left) and the summed vegetated areas and urbanised area (right) of Msimbasi Basin. .... 47

Figure 5-23: LiDAR DTM validation results at Jangwani playing grounds..... 48

Figure 5-24: Elevation differences of LiDAR and photogrammetry DTM with GNSS measurements of the ground level..... 49

Figure 6-1: Difference between levels of LiDAR DTM and DTM 2016, Green: LiDAR DTM shows higher terrain elevation, Red DTM 2016 shows higher elevation ..... 50

Figure 6-2: Difference between maximum flood depths of LiDAR DTM and DTM 2016, Green: LiDAR DTM shows larger flood depth, Red: DTM 2016 shows larger flood depth ..... 52

Figure 6-3: Locations of water depth measurements..... 53

Figure 6-4: Maximum Flood Velocities based on model with DTM 2016 (left) and LiDAR DTM (right) ..... 55

Figure 6-5: Maximum Flood Level Comparison, Green: LiDAR DTM shows larger flood levels, Red: DTM 2016 shows larger flood levels..... 56

Figure 7-1: Oblique view of the RGB coloured point cloud of the dense tree canopy area. Ground points of LiDAR (brown) and photogrammetry (white) point clouds. Scale bar in meters. .... 59

## LIST OF TABLES

Table 5-1: Scoring visual interpretation per terrain type, for LiDAR and Photogrammetry..... 40

Table 5-2: Average measured terrain levels (Z) for LiDAR and Photogrammetry. Units in meters unless noted differently .....	41
Table 5-3: Obtained point densities for LiDAR and Photogrammetry .....	42
Table 5-4: Standard deviations Z values for LiDAR and Photogrammetry. Units in meters unless noted differently .....	43
Table 5-5: Statistics for aggregated vegetated and urban areas in the Msimbazi Basin for LiDAR and photogrammetry ground point measurements. ....	48
Table 7-1: Statistical results of LiDAR and Photogrammetry methods for the aggregated areas.....	59





## 1. EXECUTIVE SUMMARY

For numerical hydraulic models accurate and reliable terrain elevation data is a key parameter. Drones, or Unmanned Aerial Vehicles (UAVs) are getting more and more interesting to derive terrain elevation datasets and are considered suitable survey methods to derive higher accuracy and resolution terrain datasets. For instance, UAVs mounted with optical cameras can be used to obtain elevation models by means of photogrammetry post-processing including ortho-imagery. This type of UAV survey has already been used extensively in Dar es Salaam. The primary result of such a survey is a Digital Surface Model (DSM) which includes elevations of objects like vegetation and buildings. However, a DTM, which excludes elevation of objects and hence represents terrain levels only, is required for flood risk modelling assessments.

Deriving DTMs from DSMs created by photogrammetry is possible, but very challenging for areas with dense vegetation cover and for areas which are not well accessible for establishing GCP's (Ground Control Points). Main reason is that with this method it's difficult to capture representative terrain points. Aerial LiDAR commonly shows a better performance in capturing terrain points in dense vegetation areas. With the development of equipment, the LiDAR scanners are getting smaller and lighter, whereas the UAVs can fly longer and can carry more weight. All in all, making UAV LiDAR more attractive over time.

For the purpose of better understanding the performance and usability of both methods for deriving a DTM for flood modelling purposes a rigorous comparison has been performed in a case study on the Lower Basin of the Msimbazi River in Dar es Salaam, Tanzania; a highly vulnerable area to flooding which requires accurate hydraulic flood modelling for identification and design of appropriate mitigation measures.

The performance to measure ground level elevation with UAV photogrammetry and UAV LiDAR in a Sub-Saharan African context, was investigated for fourteen (14) different types of vegetated areas and three (3) types of urbanised areas in the Msimbazi Basin.

For these terrain types visual interpretation was enabled by colouring the non-ground points based on the RGB UAV imagery, providing the reader with context on the type of terrain, whereas the ground points were coloured white (photogrammetry result) and brown (LiDAR results) to demonstrate the differences in measurement results per technique. The performance of measuring the ground points with both techniques was assessed by investigating:

- Density and spatial distribution of ground points over the area;
- Correctness of ground points based on classification result and relative elevation of ground and non-ground points.

In addition to the visual assessment, statistics were calculated for all terrain types, to quantify difference in performance. These results and the results of the visual assessment of the point clouds were combined to draw conclusions on the performance of both techniques to measure ground points in these terrain types. Besides this, the terrain types have also been aggregated into larger typical land use zones in order to provide practical information how LiDAR or Photogrammetry obtained ground point clouds can be interpreted and evaluated to improve processing into suitable, basin wide covering DTMs for flood risk modelling purposes.

To demonstrate the order of impact of using different DTMs for flood modelling assessments, the LiDAR DTM obtained in this Study and an earlier obtained DTM in 2016 have been used in separate simulation runs while keeping the other model parameter settings the same. Effects on flood hazard indicators like flood extent, flood levels, inundation depths and flow velocities are presented and show significant differences, underlining the importance of using accurate DTMs for this purpose.

The visual assessment is very illustrative for the performance of both techniques in the different terrain types. The urbanised areas show equal performance of photogrammetry and LiDAR. For this type of areas photogrammetry is the more favourable and cost effective technique from an acquisition and results perspective. The vegetated areas, however, show large differences in the ability to obtain ground points. This is most clearly visible for areas with mangroves and dense trees, where almost all ground points coincide with the tree canopy when using photogrammetry, whereas LiDAR penetrates the canopy and renders reliable, spatially well distributed ground points. Ground elevation differences between the two techniques can be as extreme as 5-10 m. Combined with the quantitative statistical analysis results, it can be concluded that differences decrease with lower and less dense vegetation and are on average in the order of 0.5 to 1.0 m. However, certain types of vegetation still show average elevation differences in the order of 2.0 m, like long reed and the silvery green vegetation. In all cases, LiDAR ground points in vegetated areas measure a considerably lower ground level than photogrammetry, with a better (spatially uniform) distribution over the area. Also, the standard deviation of the LiDAR ground points is considerably lower than photogrammetry, indicating a more consistent and reliable measurement of the ground level by LiDAR.

The statistical results for the aggregated areas show how much the terrain levels of Photogrammetric derived DTMs differ from LiDAR derived DTMs for a basin wide scale. Average absolute terrain levels for dense medium tall vegetated areas (2-4m height) are more than 1 meter higher with Photogrammetry compared to LiDAR; for mangrove areas the terrain levels are almost 3 meters higher with Photogrammetry compared to LiDAR. It's considered these differences can have large impacts on flood modelling outcomes. On the other hand, for urban areas, bare soil and agricultural land the differences in absolute terrain levels for both methods are marginal.

Although the LiDAR UAV survey conducted for this study was more expensive at the date of this report, LiDAR UAV is considered a more suitable method for DTM generation for flood modelling purposes in Msimbazi type of basins with relatively large coverage of vegetation with variation in type of vegetation, density and heights. Removing the uncertainties in an early stage at a higher initial cost will easily get paid off in the subsequent study and design stages by avoided additional study time and delays, and limitation of need to over-dimension designs of measures (increased cost-efficiency).

Based on the study results, the following recommendations are given:

- First assess typical terrain cover in case of considering acquisition methods for generation of DTMs for the purpose of flood modelling. This can be done by analysing satellite, ortho-imagery and drone flight imagery, and subsequently identified coverage with the results and corresponding recommendations in this study;
- In case a project requires i) hydraulic flood modelling, ii) has to deal with relatively large coverage of high and/or dense vegetation in flood plains, iii) initially had data poor conditions and iv) when a complete baseline dataset is required, it is strongly recommended to conduct UAV LiDAR survey instead of UAV Photogrammetry;
- Based on this study, for monitoring of morphologically dynamic river systems recurrent UAV Photogrammetry surveys are considered sufficiently accurate.

## 2. BACKGROUND

Dar es Salaam is getting increasingly vulnerable to river flash flooding, due to challenges including rapid and largely uncontrolled growth with weak urban and land use planning, little information to assess vulnerability and risk, and a widening infrastructure gap.

This project particularly focusses on the Msimbazi River and its tributaries which flow through the heart of Dar es Salaam, the commercial capital of Tanzania. In the middle and lower reaches of this river the city’s most severe flooding takes place, putting residents, livelihoods, properties, and critical infrastructure at risk after heavy rainfall.

Numerical hydraulic modelling is required to identify the magnitude of flood risk including its hotspots to subsequently identify and test appropriate protection and mitigation measures. For such models accurate and reliable terrain elevation data is a key parameter. For the Msimbazi River Basin a hydraulic flood model was set up in 2017, in which a Digital Terrain Model (DTM) with a spatial resolution of 5m was incorporated. This DTM was obtained through photogrammetry of aerial imagery from 2016 (hereafter called ‘DTM 2016’; ref [4]).

This model adequately served the purposes at that time. It formed the scientific basis of a Msimbazi Strategic Development and Management Framework (MSDMF; ref [1]), published in Jan 2019, which was designed to reduce flood risk. As part of the MSDMF a Detailed Plan has been developed for the lower basin of the Msimbazi valley (see Figure 2-1; ref [2]).

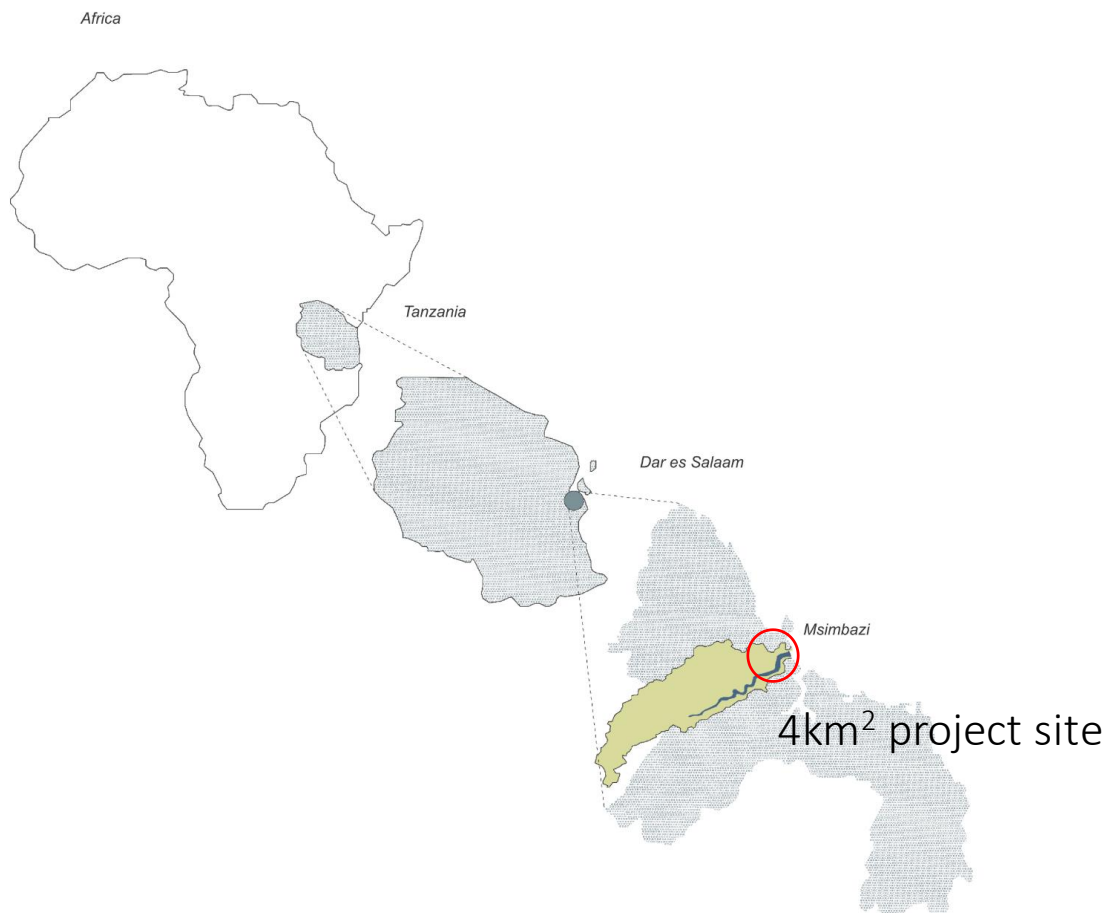


Figure 2-1: Spatial context of the Detailed Plan area of the MSDMF, which is the Study area for this Project

At times of writing this report the Detailed Plan has to be further developed into Detailed Designs and Studies for implementation of the planned interventions. In order to be able to provide the necessary higher levels of detail, the DTM of the hydraulic flood model needed to be updated with a higher accuracy and resolution.

Drones, or Unmanned Aerial Vehicles (UAVs) are getting more and more interesting to derive terrain elevation datasets and are considered suitable survey methods to derive higher accuracy and resolution terrain datasets. For instance, UAVs mounted with optical cameras can be used to obtain elevation models by means of photogrammetric post-processing including ortho-imagery. This type of UAV survey has already been used extensively in Dar es Salaam. The primary result of such a survey is a Digital Surface Model (DSM) which includes elevations of objects like vegetation and buildings. However, a DTM, which excludes elevation of objects and hence represents terrain levels only, is required for flood risk modelling assessments.

Deriving DTMs from DSMs created by photogrammetry is possible, but very challenging for areas with dense vegetation cover and for areas which are not well accessible for establishing GCP's (Ground Control Points). The Msimbazi Lower Basin is facing these issues. The flood planes are low lying wet areas, covered with vast areas of tall grasses and reed as well as dense mangrove vegetation close to the outfall of the Msimbazi River.

Commonly known, traditional aerial LiDAR acquisition methods by planes can better capture terrain elevation with ground-independent positioning systems (RTK-GNSS and INS), and are therefore more suitable to derive high quality DTMs in these challenging areas. With the development of equipment, the LiDAR scanners are getting smaller and lighter, whereas the UAVs can fly longer and can carry more weight. This potentially provides significant cost savings compared to both traditional aerial LiDAR and field surveying methods. However, compared with a UAV photogrammetry survey, a UAV LiDAR survey still costs about 2 to 3 times more. A meticulous comparison between UAV photogrammetry and UAV LiDAR, especially for a Sub-Saharan African context, is lacking. That makes it difficult to assess which UAV survey acquisition method is to be adopted for a specific case.

Therefore, in line with the innovative nature of the Tanzania Urban Resilience Program (TURP) data collection methods, a drone equipped with a LIDAR system was utilized over the Msimbazi Detailed area Plan. This way two purposes were served; i) generation of reliable, accurate and fit for purpose data for the next phases for implementation of the MSDMF and the probabilistic flood model, and ii) rigorous comparison of DTM generation by different drone acquisition methods, viz. UAV Photogrammetry and UAV LiDAR including advise on when to apply which acquisition method. This report presents the results of the latter purpose of the survey.

### 3. INTEGRAL SURVEY CAMPAIGN

The comparison analysis which forms the basis of this report is based on data obtained from an integral survey campaign. A survey is considered integral when the survey generates a complete set of data and information which serves a specific purpose; in this case setting up a detailed numerical hydraulic flood model. An integral survey is also characterised by i) simultaneous execution of different survey components (synchronicity), that ii) one and the same positioning system is used for all spatial survey components, and that iii) spatial data and information is referenced to the same horizontal and vertical reference systems.

#### 3.1 Study area

The project area is the lower basin of the Msimbazi River valley at the outfall into the Indian Ocean. In this area two tributaries (The Sinza River and the Kibangu River) merge with the Msimbazi River. The valley is characterised by a large floodplain which is bordered by a scarped natural slope to higher terrain levels. The higher grounds also approximate the demarcation of the study area as the lower grounds are prone to flooding. The larger share of the floodplains area is covered with (wetland) vegetation, but is also crossed by road infrastructure, a large bus depot and urban areas particularly in the southern reaches of the Study area.

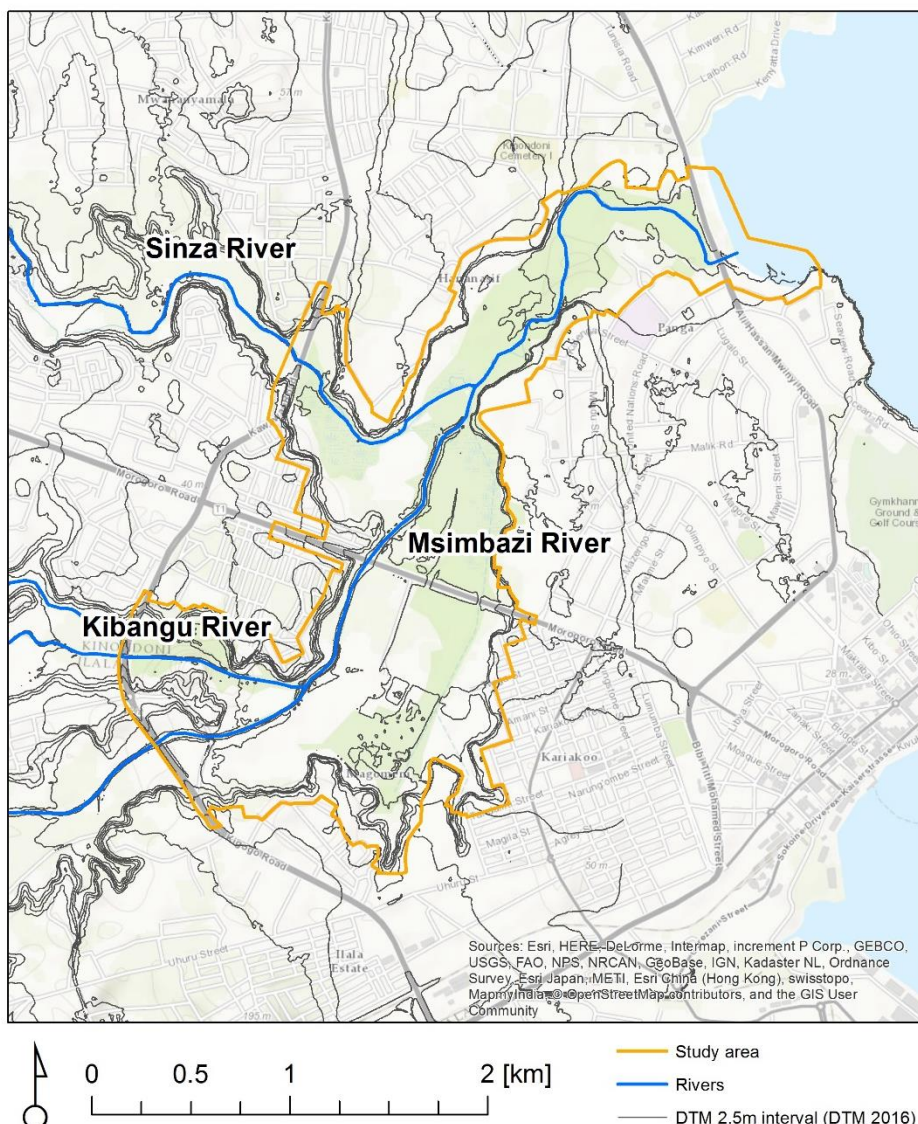


Figure 3-1: Study area

### 3.2 Survey Components

The envisioned usage of the survey data determines the survey data requirements. One of the main components of a hydraulic flood model is the DTM. Water flows from higher to lower places and open surface water manifests horizontally. In that respect, the absolute and the relative terrain elevation level variation is extremely important to simulate flood water flow and its properties like flow velocities, inundation depth and flood extent. Therefore, accurate and high resolution, area covering terrain elevation measurements are required.

Roughness, or resistance, is also an important hydraulic model parameter, and is largely determined by the type of terrain surface and the objects and coverage present. The higher the roughness factor in the hydraulic model, the more resistance is exerted to water flow, the smaller the hydraulic capacity of that river section could be. Roughness can vary between different vegetation types and surface coverages, hence it is necessary to map the land coverage to a classification which differentiates the relevant roughnesses in the project area. In case of vegetation, the density, shape and height of the vegetation determine the roughness index.

The above described survey data requirements for hydraulic flood modelling purposes can be met by measuring bed levels (bathymetry), terrain levels (topography), river water levels and orthophoto imagery to enable adequate validation and calibration of the model.

The following survey activities were proposed and executed:

#### 1 - Setting out Reference Points

Reference points were set out for use as benchmarks and ground control points for referencing of the data products. It is considered very important that all survey measurements are reduced to one and the same horizontal and vertical reference system, viz. WGS1984 UTM Zone 37S and EGM2008 respectively.



Figure 3-2: Setting out Ground Control Points and Benchmarks

#### 2 - Bathymetric survey

The river bed levels have been measured in two ways; 1) river transects every 200m with RTK-GNSS by foot with a survey pole for the parts where the river was shallow enough to cross by foot, and 2) a Single Beam Echo Sonar & RTK-GNSS survey for the river sections close to the outfall which are too deep and need to be surveyed by boat.



Figure 3-3: Two left images showing the SBES bathymetric survey and the image right showing the RTK-GNSS survey by foot

### 3 - Topographic survey

Topography was measured with two methods, namely UAV photogrammetry and UAV LiDAR. The photo camera and the laser scanner were mounted to the same drone and for both methods data was obtained through the same flights.



Figure 3-4: Equipment configuration for both UAV LiDAR and UAV Photogrammetry

### 4 - Water level and conductivity measurements

A water level logger was installed underneath the Selander Bridge at the outfall of the Msimbazi River to measure water levels and conductivity (salinity) for a period of at least one month. Also, and especially here, vertical referencing of the installed water level logger was considered very important to link the levels to the terrain heights.

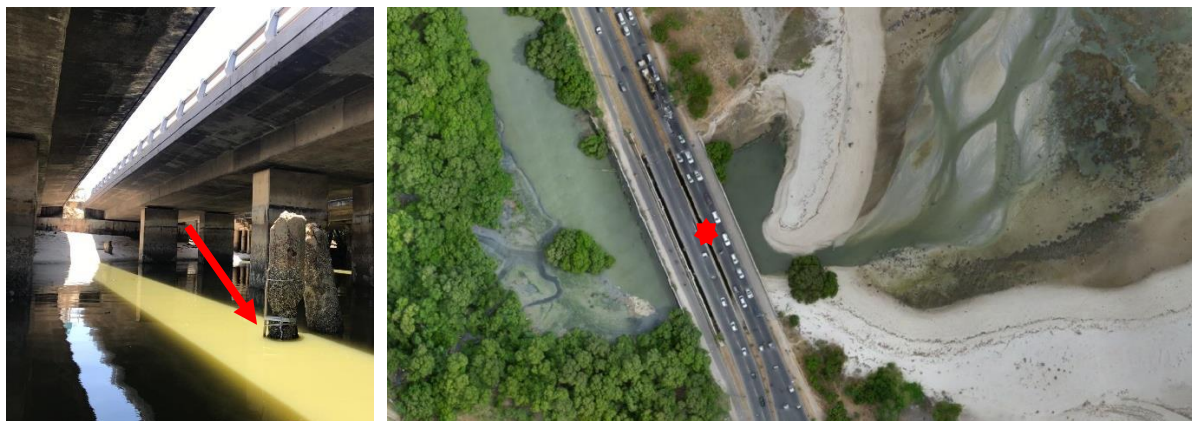


Figure 3-5: Location of installed water level logger underneath Selander Bridge

The entire survey campaign took place from 14<sup>th</sup> until 20<sup>th</sup> of February 2019. Only the retrieval of the water level logger was done after this period. For the full details of all equipment used for this integral survey reference is made to the Field Report (ref [3]).

## 4. COMPARISON OF UAV LIDAR AND UAV PHOTOGRAMMETRY FOR DTM GENERATION

### 4.1 Principles of measurement techniques

#### 4.1.1 Photogrammetry

Photogrammetry uses triangulation techniques to derive the position and elevation of an object seen (photographed) from at least two different positions and angles, based on matching pixels in the overlapping images. It is a derivation or reconstruction technique and not a direct measurement.

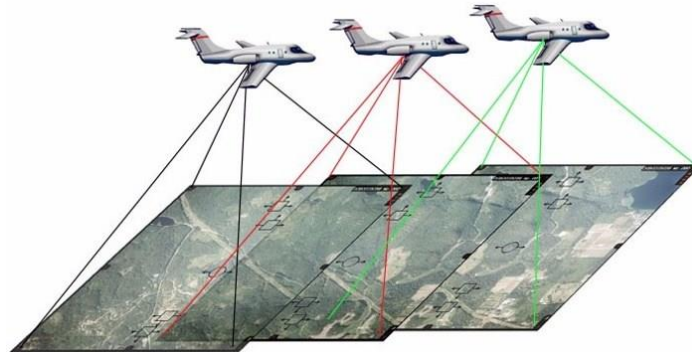


Figure 4-1: Overlapping aerial images taken from different positions and angles form the basis for generation of DTMs by Photogrammetry

Fundamental to realize: the derived elevation of the reconstructed area with photogrammetry is the elevation of what is visible in the images. If the ground is not visible, there is no possibility to derive its elevation on that location based on images.

Overlap of the footprint of - and contrast in the aerial images is needed to be able to triangulate an object on the ground. Generally, overlap in image footprint along the flightpath (60 to 80%) and across the flightpath (40 to 60%) is necessary to get good position and height approximations of the surfaces visible in the picture. These triangulation results are called *tie points*. Software packages like Agisoft Photoscan or Pix4D are built around this principle and aim at triangulating not only objects, but individual pixels in overlapping images. Algorithms seek to correlate pixel pairs in an iterative process of the estimated camera position and orientation (of the drone) and overlapping footprints of the images. Generally the more overlapping pictures and the more contrast in the images the more pixels are tied together in space to form an initial raw point cloud in x,y,z coordinates.

These software packages optimize the tie points, camera positions and camera parameters (internal and external, viz. principle points, distortion etc.), based on input by the processor, of which are considered most fundamental:

- Ground control points, to relate the tie points to real world coordinates and force accuracy and scale to the model of tie points. This tells the model: this is the real world position of these pixels; use them to scale the other tie points.
- Estimated coordinates and accuracies of the camera position and orientation, which determines from where an object on the ground is captured and triangulated from the images. This helps the model with the iterative process to tweak camera position and -parameters in such a way that all triangulated pixel pairs form a coherent model and still fit on the ground control points. What happens in between these points is pure mathematics and reconstruction (not measuring).

More and more drones are fitted with RTK-GNSS sensors (still widely varying in accuracy) to get an initially good camera position, which requires less ground control point measurement in the field.

These are however always necessary to accurately georeference the results and minimize artificial distortions in the models, due to camera parameters. Note: most drones are not fitted with geometrically calibrated cameras, which would not require optimization of the camera parameters since they are fixed and calibrated to start with.

#### 4.1.2 LiDAR

LiDAR (Light Detection and Ranging) is a technique to measure objects and areas using laser (light). Critical components of a LiDAR system are the:

- Laser scanner, which sends out laser beams and receives them back after they have reflected on the surface of an object or area. The time between sending out a laser beam and receiving it back at the sensor is recorded, multiplied by the speed of light and divided by 2 to derive the distance between the sensor and the reflected surface. The laser scanner measures distances per laser beam in time. This is done over 700.000 times per second for the current system.
- RTK-GNSS, which records the position of the LiDAR system in space and time on a centimeter accuracy level. This is necessary to translate the distance measurements of the laser scanner to x, y, z locations in the real world.
- IMU/INS, which records the orientation of the LiDAR system in space and time on a 0.015 deg accuracy level. This is necessary to determine into which direction the laser scanner is measuring the distances from the location as measured by the GNSS. If the angle is of, the resulting measured points will be placed on a different location than they really are.

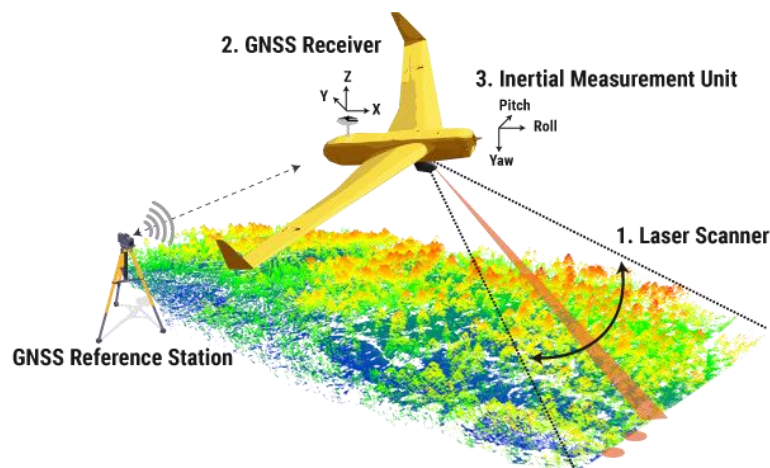


Figure 4-2: Main equipment components for UAV LiDAR to enable direct measurements

The latter two components are the most critical components for mobile laser scanning with drones. Conventional laser scanning is performed by placing a laser scanner on a perfectly level tripod, over a known marker in the ground. The distances scanned with the laser scanner are then the only variable and directly form a point cloud of the area around the scanner. The known coordinates of the marker in the ground and the height of the sensor above it, are used to position the point cloud in real world coordinates.

A drone is nothing like a tripod. It is far from static: it moves, turns and vibrates. To be able to use the laser scanner under a drone for surveying, the GNSS and IMU of the LiDAR system constantly measure the position and orientation with high frequency. An IMU that is aided with GNSS information is called an INS, resulting in even better position and orientation in time: a trajectory.

The measurements of the laser scanner and the trajectory are coupled together in real time based on timing and thereby directly measure the surrounding area with hundreds of thousands of points per second.

Moreover, the laser scanner sends out so many laser beams that while moving a part of the beams can also penetrate through vegetation and its canopies to measure the ground level. However, penetration of light through a canopy is the limiting factor in obtaining terrain levels. When sunlight can hardly reach the ground (in very dense vegetation), LiDAR beams cannot do either.

For more information on the used LiDAR system for this comparison reference is made to the Field Report [1].

## 4.2 Acquisition

### 4.2.1 Photogrammetry

Photogrammetry requires less strong, heavy drones than LiDAR, since the drone only needs to carry itself, batteries and the camera, resulting in a smaller total take-off weight. In the African context mainly fixed wing systems are used with flight ranges exceeding 100 km's per battery. The Msimbazi valley could be mapped (photographed with overlapping images) within hours and a single flight. The result of such a mapping flight would typically be thousands of images, with known (estimated) position and orientation per image location as measured with the (RTK)GNSS and IMU on the drone.

These images can be processed into a point cloud with x,y,z,r,g,b points, a DSM and an orthophoto. The accuracy of the sensors and ground control data largely determines the accuracy of the results. Depending on the systems accuracy of the (RTK)GNSS and IMU, amount and spread of ground control points that need to be placed and measured with (RTK)GNSS can be estimated to ensure accurate georeferencing of the photogrammetry products.

It is the groundwork that is time consuming and introduces uncertainty when temporary ground control points need to be placed and measured. It is often challenging to establish ground control points in areas which have no fixed structures or surfaces. Typically, these areas are natural areas like beaches, wetlands, intertidal areas, bushes, etc.

A second aspect one needs to realize is the need for sharp images with contrast, needed for triangulation processing in the photogrammetry software. Furthermore, this method has the following challenges but not limited to;

- Mapping of homogeneous land use areas like grasslands and forests, having less contrast in the images;
- Movement of vegetation due to e.g. wind, resulting in different positions of the same vegetation objects in the paired images;
- Highly reflective surfaces like open water making it difficult to match pixels.

### 4.2.2 LiDAR

LiDAR systems are still heavy in the world of commercial UAV's. The system used for this comparison weighs 3.5kg. Together with the multi-rotor drone (DJI M600pro) the total take-off weight is just under 15 kg. At the time of writing this report, this is one of the most fundamental differences in terms of acquisition. Where photogrammetry fixed wings are made to stay up in the air for hours and cover hundreds of flight line kilometers per flight, the multi-rotor with the LiDAR systems can perform flights of 13-15 minutes, after which batteries need to be changed and therefore the drone has to come home and land (in a controlled way) regularly. This is very demanding for the logistics on the ground and requires thorough relocation planning prior to the mission.

The Msimbazi Valley survey was performed from 7 different home locations throughout area, which all needed to be assessed on appropriateness, security and possibility to get permission from local leaders of the area.

A very positive aspect about the LiDAR survey acquisition, is real time control on the measurement of the area. Because it is a direct measurement technique, the results can be monitored in real time via WiFi/3G/4G connection with the system on a field laptop (or even from a computer in an office 3G/4G only).

Secondly, because all components that determine the accuracy of the final point cloud are attached to the drone, there is no need for ground control points, saving a lot of time. Common practice is to measure a few 3D objects within the area with RTK-GNSS, to perform a planimetric and height check on the point cloud.

A disadvantage of LiDAR acquisition techniques is that it does not capture highly reflective surfaces adequately, like open water bodies.

## **4.3 (Post)-processing to DTM**

### **4.3.1 Photogrammetry**

Processing principles were already briefly described in section 4.1.1. This section focusses on the steps after initial triangulation of tie points.

To further optimize the initial tie point cloud, markers are placed on the image pixels of individual images which correspond to placed and carefully measured (x, y, z) ground control points in the field. The marker's pixel coordinates (often referred to as u,v coordinates) are now related to real world coordinates (x, y, z). By placing markers on all images that have pixels with visible ground control points, the tie point cloud (initial triangulation result) is optimized (real scale and coordinates are introduced into the model), camera positions are optimized (iterative) and camera lens parameters are optimized. Optimized meaning: getting a mathematically better solution (convergence) for the relation between real world markers, pixel coordinates, camera positions and camera lens parameters.

After this step, the pixels in overlapping images that were initially not triangulated, are now assigned an x, y, z coordinate, based on relations obtained through optimization as just described. The resulting point cloud is often called the dense point cloud (e.g. in Agisoft Photo Scan, Pix4D, etc.). It is important to realize (and will become apparent later in the comparison as well) since this technique results in patches of very dense points, while other areas (which were not triangulated initially) remain absent of points.

This dense point cloud can be used to generate a mesh, DSM and orthomosaic. Either with the same software package (Agisoft, Pix4D, etc.) or with point cloud processing software, like for instance LAStools and Cloudcompare. DSM is specifically mentioned here, since the initial photogrammetry point cloud is not a reconstruction of the ground level (terrain level) in vegetated areas (where one cannot see the ground in the images). However, photogrammetry software packages have built in tools to assign points to certain classes (roads, ground, vegetation, building, etc).

Generally, the dense cloud is so dense, that the point elevation is simply averaged per grid cell. As mentioned already, an option exists to assign points to certain classes. By using these classes one can export a DTM based on only the points that belong to the class ground (and/or road etc.). Areas without these points can consequently be interpolated, to obtain full coverage of the DTM over the area of interest. The most suitable interpolation method to obtain a reliable DTM (highly dependent on purpose of DTM) is not investigated in the present comparison.

However, in general, when ground level information is lacking over large areas and/or considerable variability in ground level elevation within that area is present, the resulting DTM will not describe the real terrain level reliably.

Note: the more uniform the spatial distribution of ground points is over the area of interest, the more reliable and accurate the basis will be to derive the resulting DTM. Be it through interpolation, or through averaging the points per grid cell.

An alternative way to cope with vegetation is to correct for vegetation height, by means of mapping typical vegetation areas, assuming a constant height offset between top of the vegetation (DSM) and the ground level per class and correcting for it. One must be very careful with and transparent about the corrections performed on the initial DSM to derive the DTM, for it to be of any objective value for modelling purposes.

The photogrammetry software packages are commonly used to derive a DSM or DTM. For a fair comparison between photogrammetry and LiDAR, the photogrammetry dense point cloud is not processed further in the photogrammetry software, but with LAStools, just as the LiDAR point cloud.

Therefore, the photogrammetry point cloud (with all points resulting from initial triangulation up to optimization and dense point cloud generation) is exported as a .laz file (same as point cloud for LiDAR). The point cloud is automatically denoised (removal of isolated points) and classified with LAStools to classify ground and non-ground points. The DTM is derived by averaging only ground points to regular grids with several resolutions. Therefore, no interpolation is performed. Each grid cell with a certain horizontal surface (resolution) is assigned the mean of the resulting ground points (DTM) or ground & non-ground points (DSM). Results of the ground classification and resulting DTM are presented in Chapter 5.

### 4.3.2 LiDAR

The LiDAR point cloud is a result of combining the measurements of individual sensors based on timestamps in the data. It concerns the following sensors:

- Laser scanner;
- GNSS;
- IMU.

The scan angle or field of view (FOV) of the laser scanner can be set from 0 (no data) to 360 degrees (data from each full spin cycle of the laser scanner). Generally, only the down looking part of the circle is used and formulated on either side of nadir. Meaning a scan angle of 50 degrees results in a FOV of 100 degrees (centred on nadir). For this system any of the 32 lasers can be selected to use in post processing, rendering different point densities of the initial point cloud. For this project 16 (out of 32) lasers were used to construct the point cloud. The used laser scanner (Velodyne HDL 32e) gives 2 returns per measurement. The last return is used for ground point classification.

The GNSS and IMU data was post processed with Inertial Explorer to derive the most reliable trajectory of the drone (and laser scanner). This trajectory was also used to provide the photos with accurate positions for the photogrammetry processing.

Flight lines were automatically analysed to isolate the actual planned flight lines (without the turns in between them). The result is a point cloud in real world coordinates. The points do not have colours yet, since they were derived with the laser scanner and not with a camera. They can be coloured either by projecting the individual images onto the point cloud, or by colouring the point cloud with the orthophoto derived with photogrammetry. The latter is done for this comparison.

The noise filtration is executed with LASnoise.exe, a tool which flags noise points according to criteria that can be modified by adjusting the -step and -isolated parameters. With -step the x, y and z size of the cells is set and with -isolated the least amount of points that can be present in a cell is set. If there are less points in the cell than the -isolated value, they are flagged as noise.<sup>1</sup>

The ground determination is executed with LASground.exe<sup>2</sup>. This tool classifies points into ground and non-ground points, based on user defined settings. The point cloud was divided into the two dominant landuse types: urbanized and vegetated areas. Both were classified by LASground.exe but with different parameters. For the urban area the -town preset has been used and for the vegetation area the -nature preset.

The classified point clouds (denoised and ground/non-ground) were exported to digital terrain and surface models with BeamWorx Autoclean. No interpolation was performed, grid cells with datapoints were assigned the mean elevation of the classified points. The resulting grids were visualized and compared in GIS software. Empty cells were left empty.

The photogrammetry and LiDAR pointclouds were processed identically in LASTools and BeamWorx, for a fair comparison. Results of the ground classification and resulting DTM are presented in Chapter 5.

## 4.4 Data comparison methodology

### 4.4.1 Introduction

The performance to measure ground level elevation with UAV photogrammetry and UAV LiDAR in a Sub-Saharan African context, was investigated for fourteen (14) different types of vegetated areas and three (3) types of urbanised areas in the Msimbazi Basin (see Figure 4-3).

Areas were selected based on different types of land use, viz. vegetation type (density, height), spatial distribution of vegetation (single tree or dense agglomeration of trees), bare ground, agricultural grounds and urbanisation.

The derived photogrammetry and LiDAR point clouds form the basis for the analysis. Both point clouds were classified in ground and non-ground point classes, using LASTools. Point clouds with the non-ground points were coloured based on the RGB UAV imagery, providing the reader with context on the type of terrain. Point clouds with the ground points were coloured white (photogrammetry result) and brown (LiDAR results) to demonstrate the differences in measurement results per technique.

The point clouds of both techniques were visually assessed on:

- density and spatial distribution of ground points over the area;
- correctness of ground points based on elevation.

Ground point cloud statistics for photogrammetry and LiDAR were calculated for each area. Statistics and results of the visual assessment of the point clouds were combined to draw conclusions on the performance of both techniques to measure ground points in these terrain types.

---

<sup>1</sup> [http://lastools.org/download/lasnoise\\_README.txt](http://lastools.org/download/lasnoise_README.txt)

<sup>2</sup> [http://lastools.org/download/lasground\\_README.txt](http://lastools.org/download/lasground_README.txt)

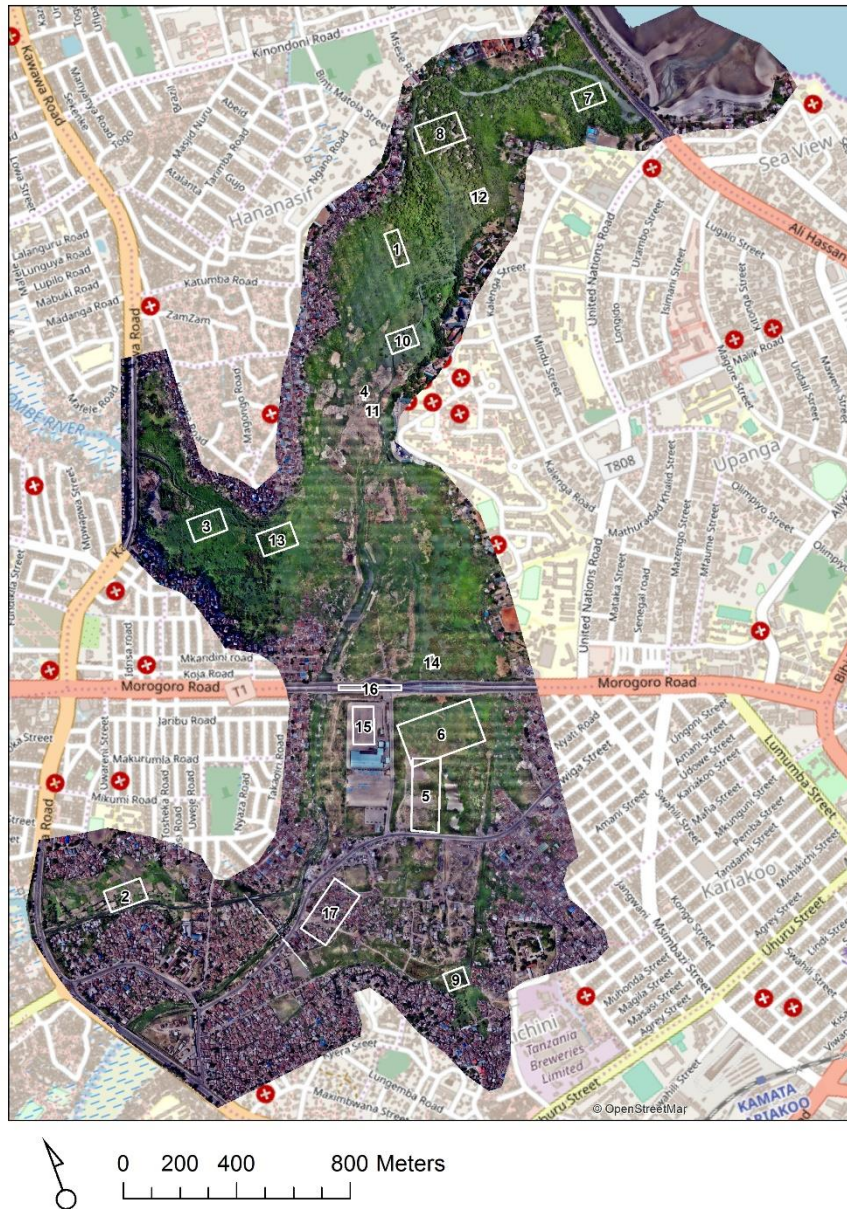


Figure 4-3: Location of assessment areas (red) on background of orthophoto and OSM

The assessed vegetated areas were aggregated into representative areas in the vegetated part of the basin to derive more generic results in relation to benefits and consequences associated with both techniques and the corresponding percentage of these areas relative to the total basin. Vegetation height and density form the basis for the aggregation. Conclusions were drawn by combining the statistics of the terrain types, visual inspection of the performance to measure ground points and aggregating them to representative areas of the Msimbazi Basin.

A last step in the comparison of both techniques was validation of the DTMs with GNSS validation data (ground truth) obtained at Jangwani playing grounds.

#### 4.4.2 Selection of typical terrain types

Fourteen (14) types of vegetated areas and three (3) types of urbanised areas in the Msimbazi Basin (see Figure 4-3) were selected based on land use, viz. vegetation type (density, height), spatial distribution of vegetation (single tree or dense agglomeration of trees), bare ground, agricultural grounds and urbanisation:

1. Separated dense bushes alternated with low vegetation
2. Crops, trees and agricultural grounds
3. Dense, medium tall vegetation
4. Single bush and dwelling with bare ground
5. Jangwani playing grounds
6. Bush, short grass with bare ground
7. Mangroves with dense canopies
8. Mangroves with visible ground level through the (less dense) canopies
9. Flattened reed vegetation
10. Silvery green dense vegetation
11. Single tree, single bush, dense silvery green vegetation
12. Trees with dense canopies
13. Variety of dense vegetation near swampy terrain
14. Long reed, not dense
15. Bus depot
16. Morogoro road and bus stop
17. Urban area

**Separated dense bushes alternated with low vegetation (terrain type 1)** are one a common type of terrain in the Msimbazi Basin (Figure 4-4). The bushes' canopy is very dense, but with alternating less dense low grass or vegetation around them, the ground level could potentially be measured. It is also assessed whether agglomerations of these dense bushes enable measurement of the ground level.



Figure 4-4: Separated dense bushes with low vegetation, white polygon indicates assessment area.

The Magomeni area is characterised by agricultural activity, with different crops, trees and bare ground (Figure 4-5; **terrain type 2**).



Figure 4-5: Crop, trees and bare ground, white polygon indicates assessment area.

**Dense medium tall vegetation (terrain type 3)**

The Msimbazi valley is covered with large patches of dense, medium tall (2-3 m) vegetation (Figure 4-6). In this case dense refers to the number of stems and grass blades packed together per unit surface, ultimately obstructing the (sun)light to reach the ground level. Dense patches are formed throughout the valley by several different species, of which the exact names and properties were not included in this analysis. Due to the abundant presence, the ability to measure the ground level for this type of terrain is very important



Figure 4-6: Dense medium tall vegetation, white polygon indicates assessment area.

An area with a single bush and a manmade shelter with bare ground (**terrain type 4**) around it is assessed to show the similarity of measuring the ground level 'in a house' and under dense vegetation (Figure 4-7).



Figure 4-7: Single bush and manmade shelter with bare ground, white polygon indicates assessment area.

The Jangwani playing grounds (**terrain type 5**) are a typical example of the terrain coverage in the southern part of the basin, with bushes, long reet, long grass and bare ground (Figure 4-8). This area was used to obtain validation data.



Figure 4-8: Jangwani playing grounds, white polygon indicates assessment area.

In semi cultivated parts of the basis **bush and short grass with bare ground (terrain type 6)** in between is present (Figure 4-9). This type of terrain is expected to be quite favourable for both techniques to measure the ground level.



Figure 4-9: Bush and short grass with bare ground, white polygon indicates assessment area.

**Mangroves with dense canopies (terrain type 7)** are often found in (tropical) coastal areas with freshwater influences (Figure 4-10). Dense refers to the canopy, blocking sunlight to penetrate it and disabling to detect ground level in aerial images. Surveying the bathymetry and topography with GNSS is often impossible due to canopy coverage or simply the accessibility of the ground level (mud and roots). The morphology is characterised by pronounced height variability between channels and plains.



Figure 4-10: Mangroves with dense canopy, white polygon indicates assessment area.

**Mangroves with less dense canopies (terrain type 8)** were also selected to assess whether photogrammetry could measure these areas, since ground level is visible from the sky (Figure 4-11).



Figure 4-11: Mangroves with less dense canopies, white polygon indicates assessment area.

A striking type of vegetation in the basin is the **flattened reed (terrain type 9)** vegetation (Figure 4-12). It is found in the west and south(east) of the basin, mainly close to inundated areas. Stems are growing in patches, potentially enabling measurement of the ground level in between them.



Figure 4-12: Flattened reed, white polygon indicates assessment area.

The **silvery green dense type of vegetation (Figure 4-13; terrain type 10)** is observed scattered over the lower basin and more concentrated along and near the embankments of the river (eastern part mainly). This type of vegetation is less dense, though the stems have several branches, possibly obstructing measurement of the ground level. Assessment of the ability to measure the ground level for this type of vegetation is very relevant, because of the location close to the water/embankment.



Figure 4-13: Dense silver green vegetation, white polygon indicates assessment area.

The area called **single tree (terrain type 11)**, single bush, dense silvery green vegetation is assessed to show the resulting ground points under a single tree, surrounded with some bush and a patch of silvery green vegetation (Figure 4-14).

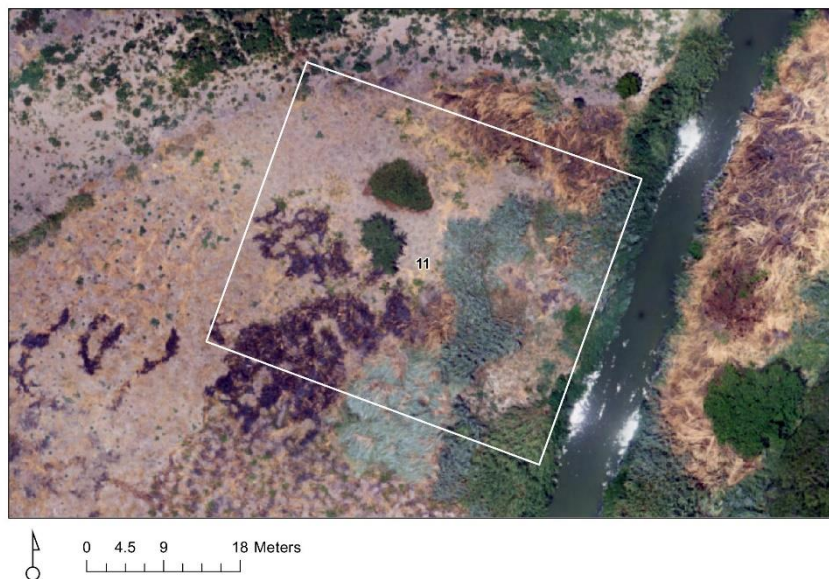


Figure 4-14: Single tree, bush and silvery green vegetation

Even though **trees with dense canopies (terrain type 12)** are expected to yield similar results as mangroves with dense canopies, this area is investigated separately (Figure 4-15). Mangroves often have a shiny, wet, though unvegetated bed level. This is certainly not the case for regular dense trees areas, where shorter vegetation types can still grow on the bed level and canopies can be even thicker. The actual underlying morphology is not predictable.



Figure 4-15: Trees dense

The Kawawa / Hanna Nassif (south) area, where the Sinza River enters the basin, is heavily vegetated. Just south of Hanna Nassif a **variety of dense vegetation near swampy terrain (terrain type 13)** is assessed (Figure 4-16).



Figure 4-16: Variety of vegetation just south of Hanna Nassif

Some of the areas are vegetated with **long reet (terrain type 14)**, which seems to be less dense than the previous described area (Figure 4-17). Possibly photogrammetry and LiDAR can measure the ground level better. The long reet can be found throughout the floodplains of the basin, making it an important vegetation class to measure the ground level accurately.



Figure 4-17: Long reed, not so dense

The bus depot (terrain type 15) is one of the main assets in the Basin and considered an urbanised area (Figure 4-18).



Figure 4-18: Bus depot

Morogoro Road (terrain type 16) and the bus stop is another key infrastructural asset in the Basin and considered an infrastructural asset (Figure 4-19).



Figure 4-19: Morogoro Road

A typical example of urbanisation in the Msimbazi Basin, prone to flooding, is shown in Figure 4-20 and considered urbanised area. (terrain type 17).



Figure 4-20: Typical urbanization, prone to flooding.

#### 4.4.3 Performance assessment

The derived photogrammetry and LiDAR point clouds formed the basis for the analysis. Both point clouds were classified in ground and non-ground point classes, using LASTools. Point clouds with the non-ground points were coloured based on the RGB UAV imagery, providing the reader with context on the type of terrain. Ground points in the photogrammetry point cloud were coloured white. Ground point in the LiDAR point cloud were coloured brown. Both are visualised to demonstrate the differences in measurement results per technique.

The point clouds of both techniques were visually assessed on the following criteria, keeping in mind that the generation of DTMs is for the purpose of flood risk modelling assessments:

- **Density and spatial distribution of ground points over the area.** Capturing terrain elevation variation is particularly important for generation of DTMs for hydraulic flood modelling, as it will determine whether certain areas will be flooded or not in the simulations. Using equally distributed ground points, opposed to using unequally distributed ground points, enhances accurateness of a derived DTM as well as its representation of terrain elevation variation over certain distances (compared for the same area and for the same amount of ground points);
- **Correctness of ground points based on classification result and relative elevation.** To investigate the ability of the techniques to actually measure points on/near the ground. When ground points are actually classified in the vegetation tops (coinciding with the non-ground points), this mainly implies that the absolute accuracy of the ground points and the resulting DTM is inadequate.

#### 4.4.4 Point cloud statistics

Quantified metrics for all 17 terrain type areas were derived through statistical analysis of the photogrammetry (Photo) and LiDAR point clouds. Parameters are:

- Surface area;
- Lowest LiDAR ground point elevation;
- Highest LiDAR ground point elevation;
- Mean LiDAR ground point elevation;
- Lowest Photo ground point elevation;
- Highest Photo ground point elevation;
- Mean Photo ground point elevation;
- Difference of the mean Photo and LiDAR ground point elevation;
- Point count of LiDAR point cloud;
- Point count of Photo point cloud;
- Difference of the Photo and LiDAR point count;
- Standard deviation of the LiDAR ground point elevation;
- Standard deviation of the Photo ground point elevation;
- LiDAR ground points per square meter;
- Photo ground points per square meter.

Results of the statistical analysis were coupled to the visual assessment of the point clouds as described in the previous section, to derive conclusions on the performance of the two methods to measure the ground level and ultimately form the basis for a reliable DTM for flood modelling purposes.

#### 4.4.5 Land use on a basin scale level

The assessed vegetated areas were aggregated into eight (8) representative areas in the vegetated part of the basin to derive more generic results in relation to benefits and consequences associated

with both techniques and the corresponding percentage of these areas relative to the total basin. Vegetation height and density form the basis for the aggregation.

Since these valleys are also partly urbanised the results of the assessed urbanised areas are aggregated as well. Finally, the ratio of the aggregated vegetated and urbanised areas relative to the total basin area is presented and discussed.

This way the performance of LiDAR and Photogrammetry is also assessed for the total project area, providing practical information how LiDAR or Photogrammetry obtained ground point clouds can be evaluated and processed into suitable DTMs for flood risk modelling purposes.

#### 4.4.6 Validation with GNSS data for typical terrain types

The area around Jangwani playing grounds was used to obtain validation data through GNSS measurement of the ground level elevation (Figure 4-21). Validation data was obtained for:

- Bare ground
- Short grass
- Long grass
- Long reed

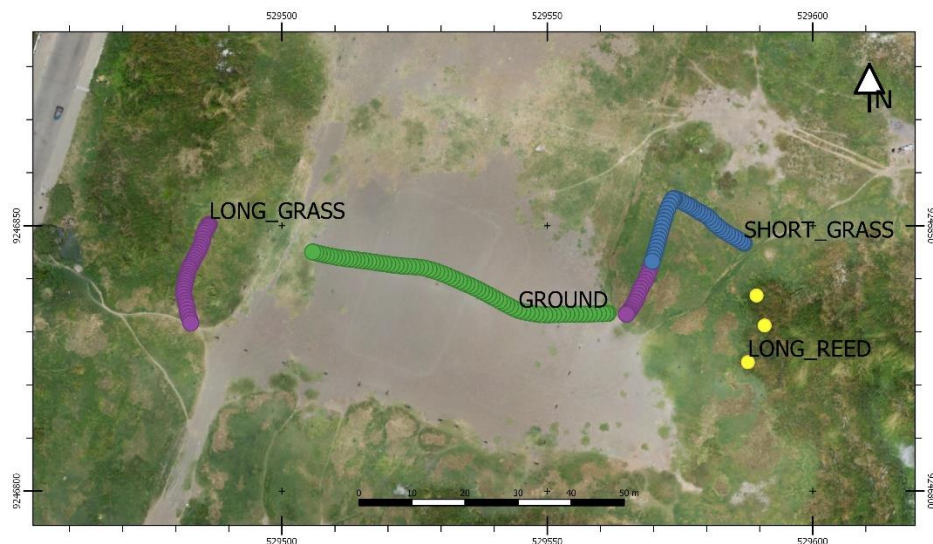


Figure 4-21: Validation points per class are indicated for bare ground, short grass, long grass and long reed.

Results were analysed by sampling the elevation level (Z) from the photogrammetry DTM and LiDAR DTM at the GNSS location and determining their difference with the measured GNSS elevation on that location. Note, the vegetation at this site was less dense and less high than in the lower (eastern) part of the Msimbazi basin. Dense bush, trees and mangroves are not present in this area.

## 5. RESULTS

### 5.1 Performance to measure ground level

The following sections show a selection of figures of the point clouds in a point cloud viewer per investigated area. Top, side and oblique views are used to (visually) present the performance of UAV photogrammetry and UAV LiDAR to measure ground points. Photogrammetry point clouds with only ground points are shown in white. LiDAR point clouds with only ground points are shown in brown. For reference of the assessed area the denoised and RGB coloured point clouds (containing all measured points) are also shown in the same figures. This provides insight into the concepts of *depth within a point cloud*, *performance to measure the ground level* and the *spatial distribution* of ground points per area. Reference is made to Appendix I for all assessed figures per terrain type.

The most striking and illustrative example of the difference in performance to measure the ground with either of the techniques is illustrated for the **dense tree canopy** areas. When viewing this area from above mainly a green canopy is observed, without ground points visible (Figure 5-1).

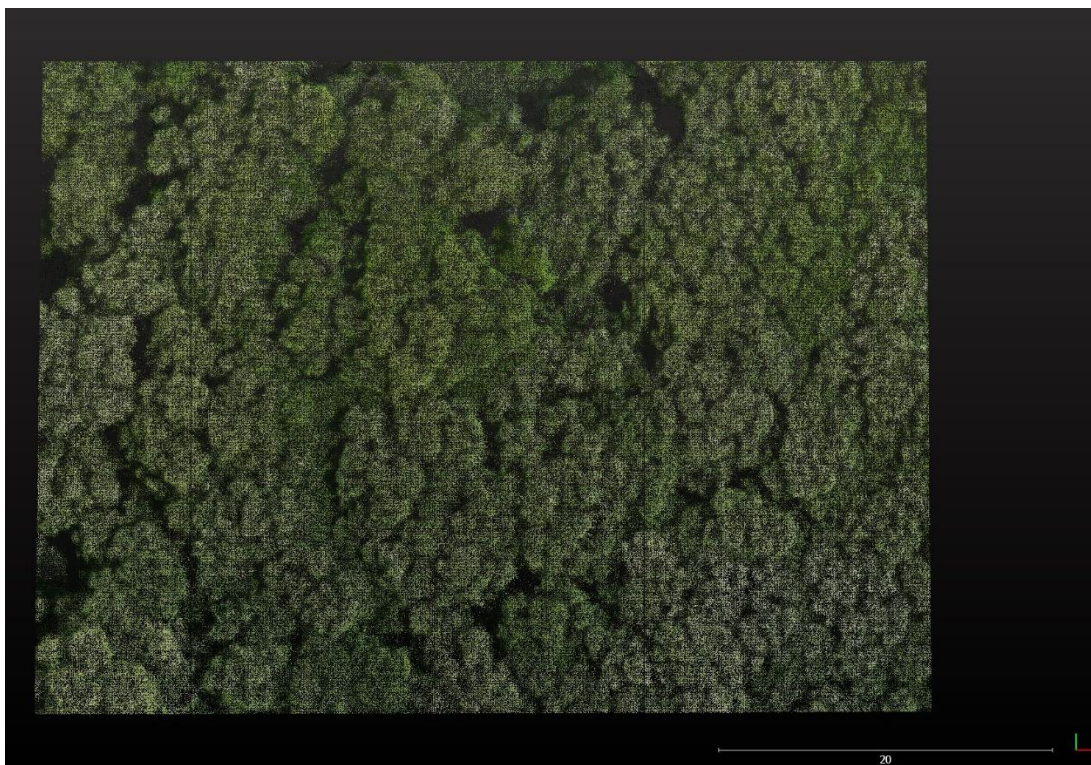


Figure 5-1: Top view of the RGB coloured point cloud of the dense tree canopy area. Scale bar in meters.

The dense canopy is also visible when looking at the point clouds from the side (Figure 5-2). The photogrammetry ground points (white) are mostly observed in the canopy and in erroneous patch of canopy which are projected close to the ground level (though still hovering above it). The LiDAR ground points (brown) clearly measure the ground level. No photogrammetry ground points are observed near in between the LiDAR ground points, from which the conclusion is drawn that photogrammetry cannot measure the ground level in this type of terrain. Instead, a blanket like cover is reconstructed over the tree canopies, whereas LiDAR actually reaches the ground below the canopy.

Considering the scale of the trees, the photogrammetry ground points ‘measure’ the ground level elevation approximately 5 to 10 m to high, depending on the height of the canopy above the ground. In other words, the relative error of photogrammetry ground points with respect to LiDAR ground points is in the order of 7.5m for this type of terrain. The statistical analysis confirms this with a value

of 7.61 m of difference between the mean of all LiDAR and the mean of all photogrammetry ground points.

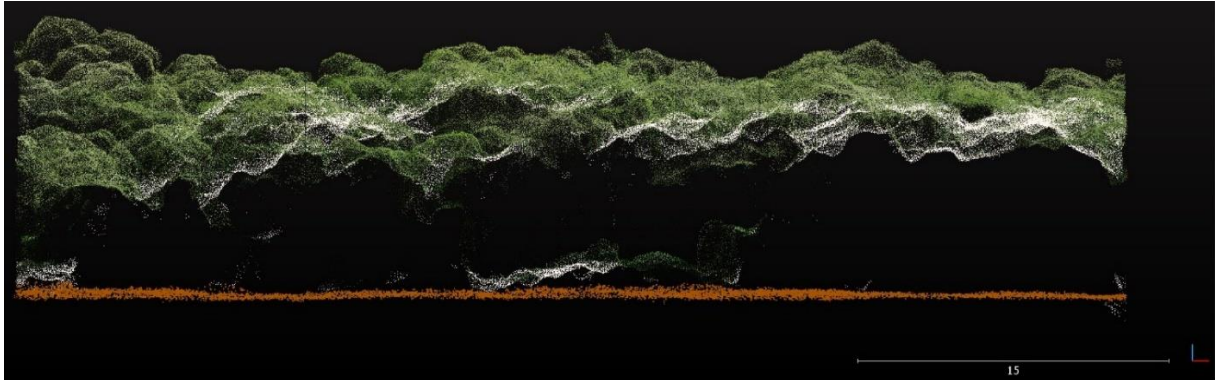


Figure 5-2: Side view of the RGB coloured point cloud of the dense tree canopy area. Ground points of LiDAR (brown) and photogrammetry (white) point clouds. Scale bar in meters.

The spatial distribution of the LiDAR ground points (brown) is assessed in the top view of the area with only ground points shown (Figure 5-3). The spatial distribution is rather uniform making it a good measurement to derive a reliable DTM for this type of area. The photogrammetry ground points are far more concentrated in patches within the areas. This lies in the principle of the technique where dense point clouds are generated around initial tie points. So, besides the erroneous measurement of the ground level, the spatial distribution is poor as well.

Note: the point count of the photogrammetry ground point cloud (~50.000) and LiDAR ground point cloud (~10.000) would suggest a better result for photogrammetry, if one doesn't take into account the spatial distribution and correctness of the ground points.

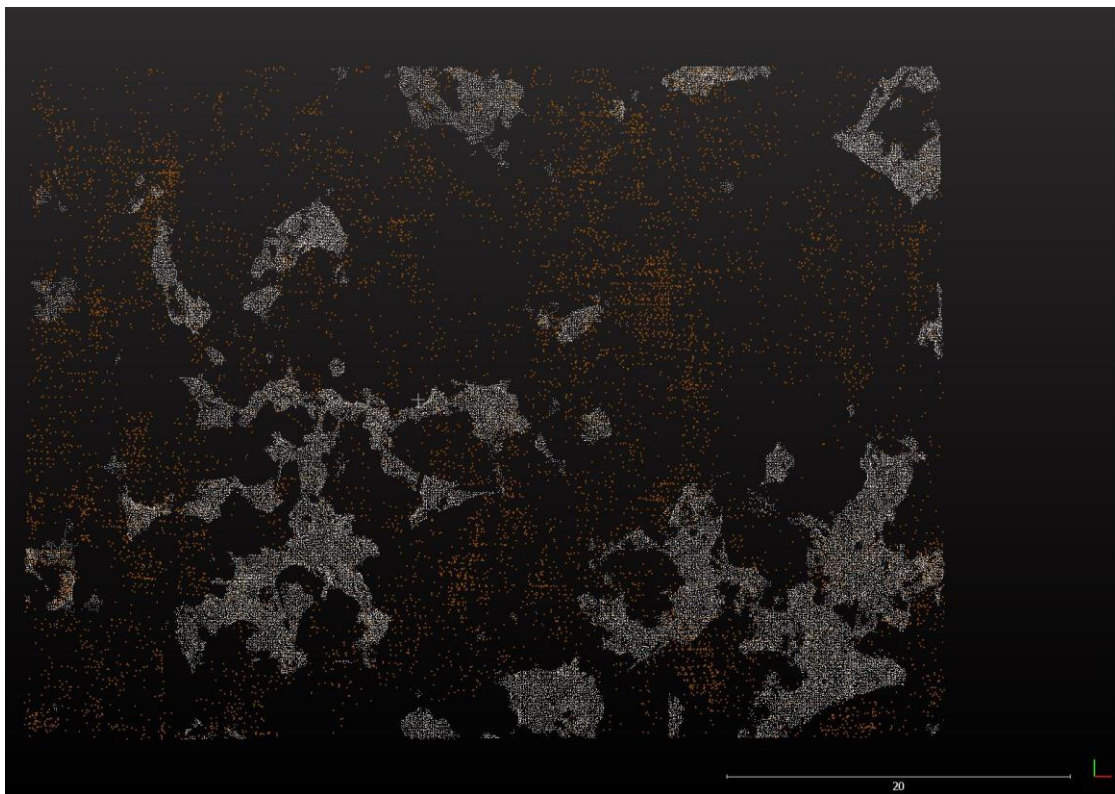


Figure 5-3: Spatial distribution of the LiDAR (brown) and photogrammetry (white) ground points. Scale in meters.

An oblique view of the point clouds is presented to illustrate the above observations once more (Figure 5-4)

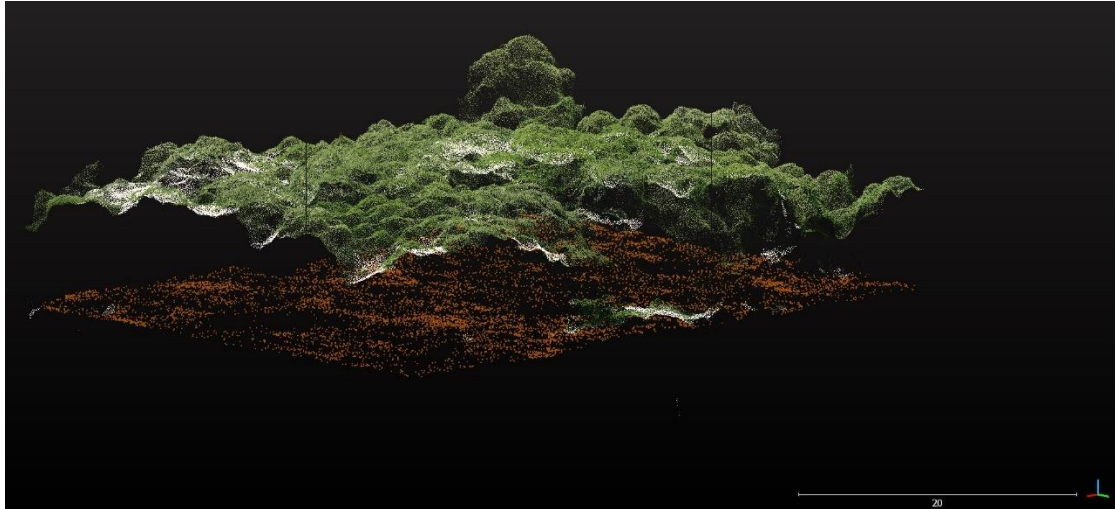


Figure 5-4: Oblique view of the RGB coloured point cloud of the dense tree canopy area. Ground points of LiDAR (brown) and photogrammetry (white) point clouds. Scale bar in meters.

From this image it also becomes apparent that correcting for a constant vegetation height correction would introduce artificial height gradients in the underlying morphology, since the LiDAR ground points show a quite uniform flat ground surface, whereas the canopy shows height variations in the order of several meters.

**Mangroves** were assessed with similar results as the dense tree area. Though due to the higher canopies and presumably the presence of shiny wet surfaces, triangulation results are poor in this area. Photogrammetry reconstructs ground points (white) below and above the ground surface as measured by LiDAR (brown). The negative ground points were, apparently, not removed as noise in the processing stage. Because patches of points are formed easily by photogrammetric dense point cloud generation, these areas can be considered isolated patches rather than isolated points.

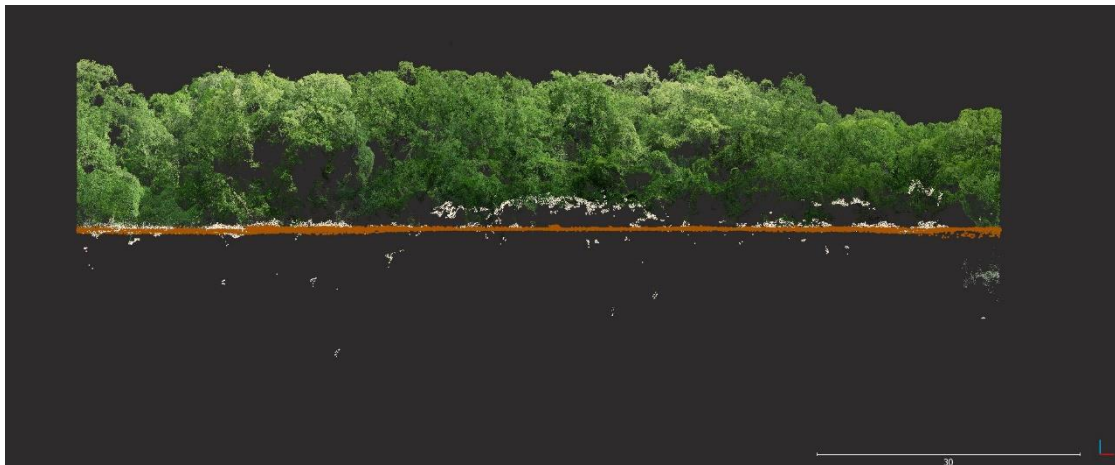


Figure 5-5: Side view of the RGB coloured point cloud of the mangroves area. Ground points of LiDAR (brown) and photogrammetry (white) point clouds. Scale bar in meters.

The results of the spatial distribution of the ground points are similar to the dense tree area. Both point clouds have approximately 30.000 points in this area, of which the LiDAR clearly covers the area more uniform than the photogrammetry patches, that also have erroneous heights.

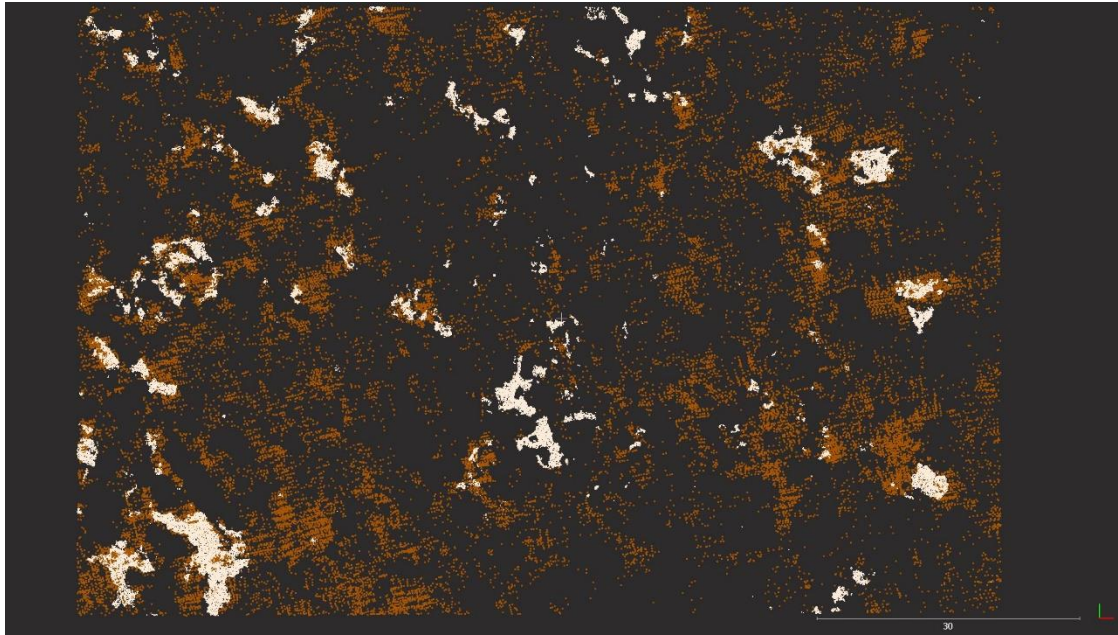


Figure 5-6: Spatial distribution of the LiDAR (brown) and photogrammetry (white) ground points. Scale in meters.

**Less dense mangroves**, with bare ground visible in between the canopies were assessed, possibly enabling photogrammetry to perform better (Figure 5-7). The results show more ground points than for the dense canopies, for both photogrammetry (white) and LiDAR (brown). The spatial distribution of the photogrammetry points is significantly less uniform than for LiDAR (Figure 5-8). The point count of the LiDAR ground point cloud (300.000) is a factor to higher than the photogrammetry point cloud (160.000) and covering the area a lot better. The correctness of the ground points is revealed in the side view of the area, showing photogrammetry points above the LiDAR ground points in the order of meters.

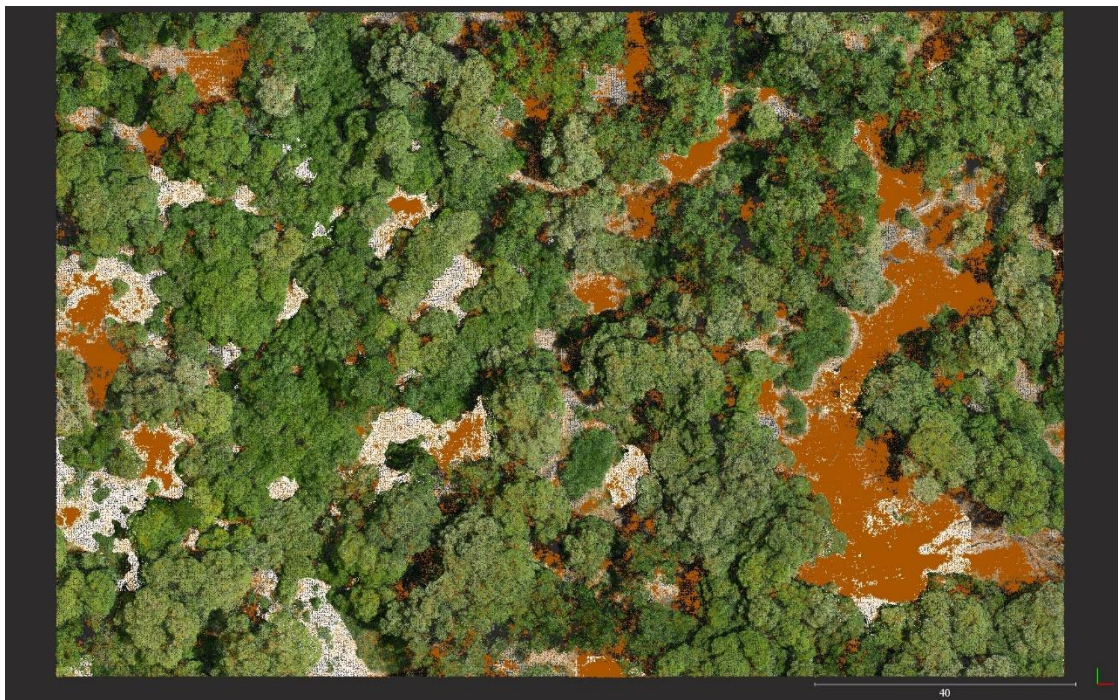


Figure 5-7: Top view of the RGB coloured point cloud of the less dense mangroves with bare ground visible. Ground points of LiDAR (brown) and photogrammetry (white) point clouds. Scale bar in meters.

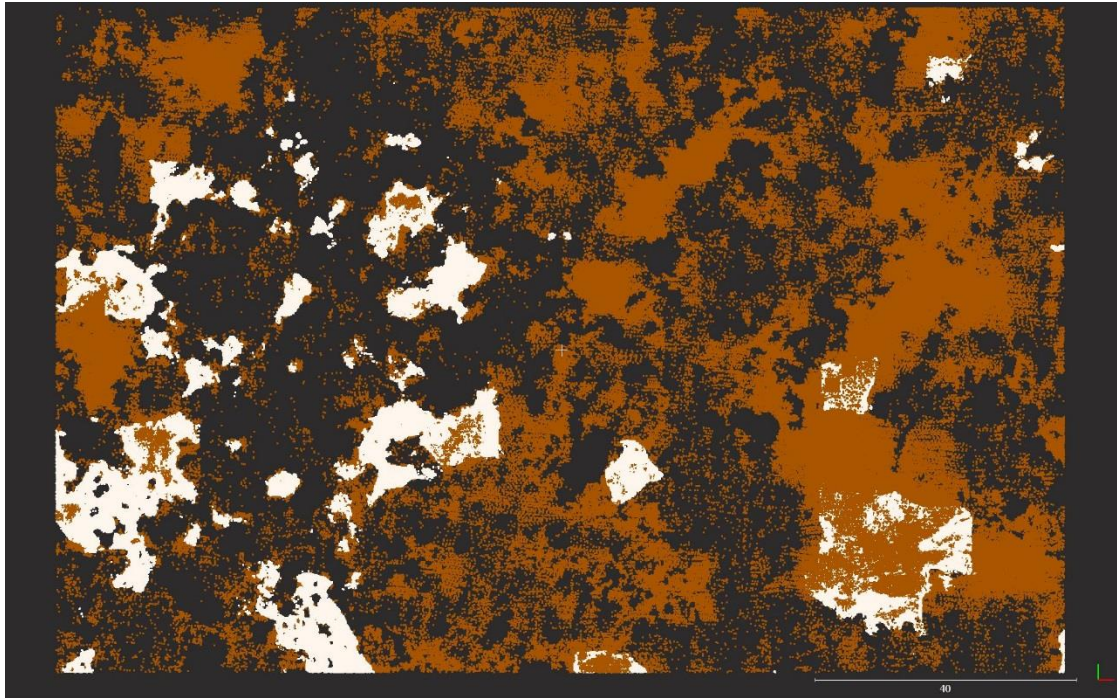


Figure 5-8: Spatial distribution of the LiDAR (brown) and photogrammetry (white) ground points. Scale in meters.



Figure 5-9: Side view of the ground points of LiDAR (brown) and photogrammetry (white) point clouds. Scale bar in meters.

Dense tree and mangrove canopies are mainly found in the northern part of the basin. Moving southward, the area is vegetated with dense bush, long reed and grass. A typical example is shown in top view by the coloured point cloud (this is not a photo) in Figure 5-10.



*Figure 5-10: Area type 10. Top view of the RGB coloured point cloud. Scale bar in meters.*

The oblique view (Figure 5-11) and side view (Figure 5-12) of this area immediately show a blanket of classified photo ground points (white) on top of the dense vegetation. The point density of this 'ground' point cloud is approximately 80 points/m<sup>2</sup>, of which almost a 100% (by visual assessment) is not actual ground. Some LiDAR ground points (brown) are visible underneath, although not many.

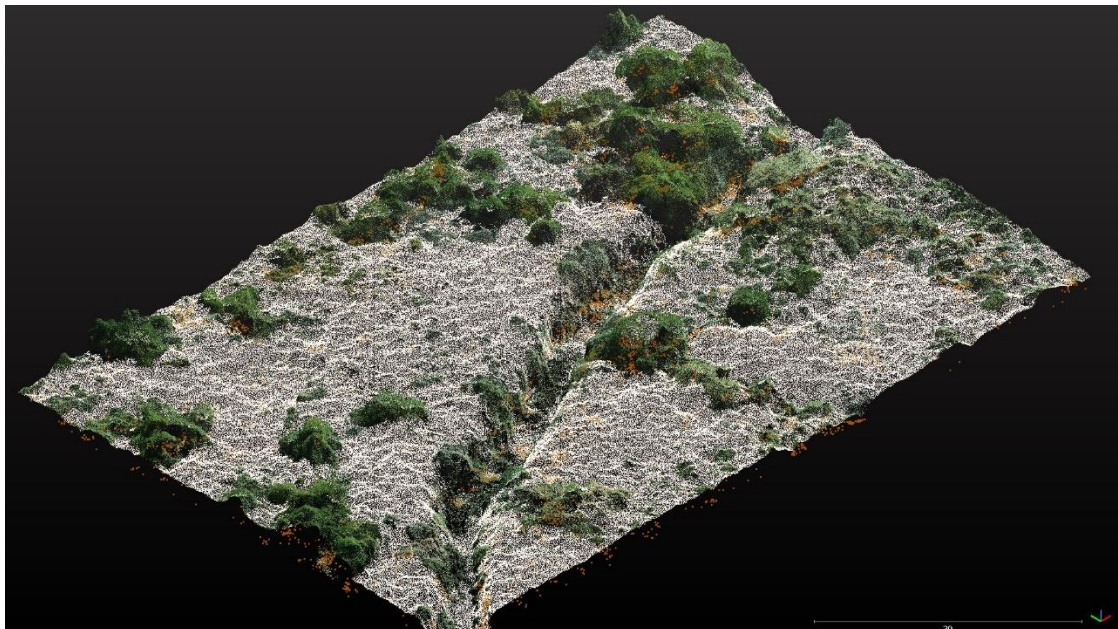


*Figure 5-11: Oblique view of the RGB coloured point cloud of the dense tree canopy area. Ground points of LiDAR (brown) and photogrammetry (white) point clouds. Scale bar in meters.*

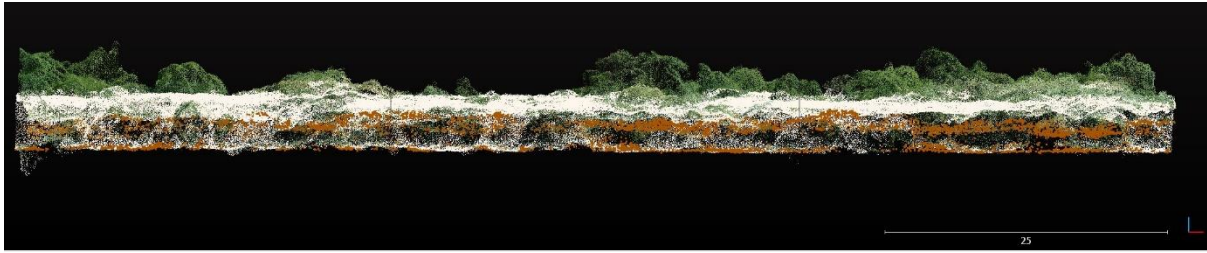


Figure 5-12: Side view of the RGB coloured point cloud of the dense tree canopy area. Ground points of LiDAR (brown) and photogrammetry (white) point clouds. Scale bar in meters.

Removing the photogrammetry ground points and RGB point cloud, reveals the remaining LiDAR ground points (Figure 5-13), which are quite evenly distributed with an average point density of 1.4 points/m<sup>2</sup>.

These images reveal the incompetence of photogrammetry to measure the ground level in this type of vegetation. However, it is hard to conclude whether LiDAR actually does measure the ground level or just penetrates the vegetation further than photogrammetry. Based on the statistical analysis it is concluded that the relative elevation error between both techniques in this area is in the order of 2 m.

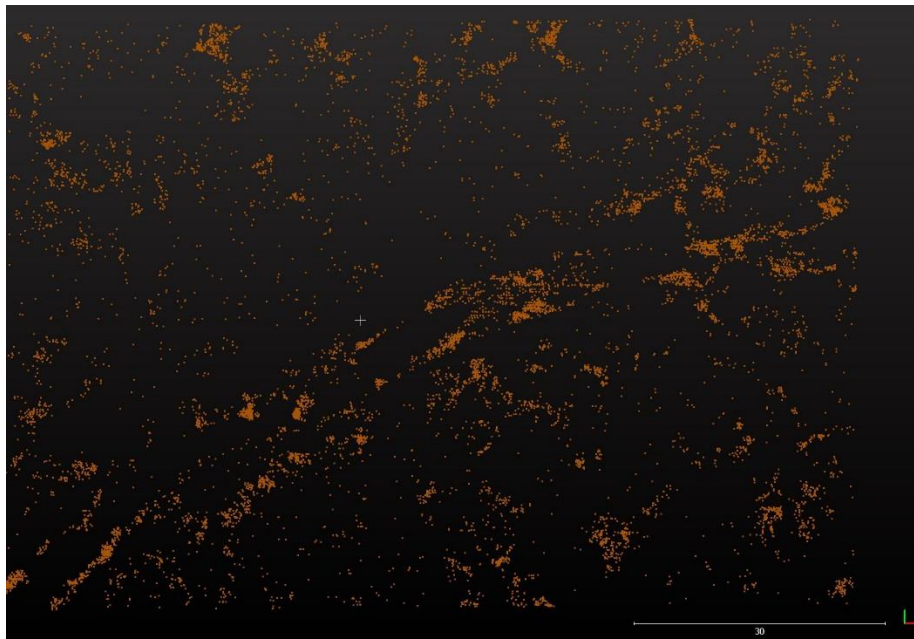


Figure 5-13: Top view of spatial distribution of the LiDAR ground points. Scale in meters.

Areas with **single trees, bushes and bare ground** in between and **semi cultivated areas** within the basin show better results for photogrammetry than in dense vegetation.(see Figure 5-14 top). However, on the dense bush, photogrammetry ground points coincide with the sides of the bushes (Figure 5-14 bottom). For LiDAR, limited ground points below the dense canopy are visible.

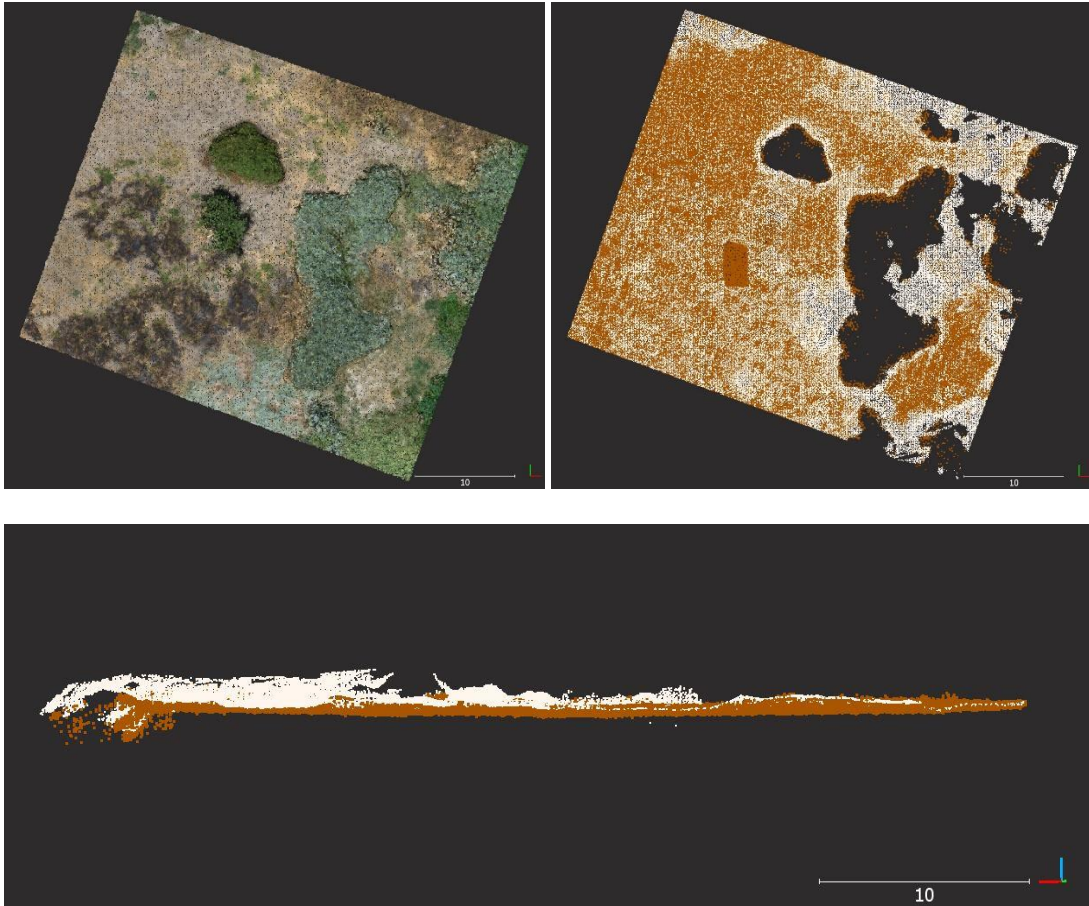
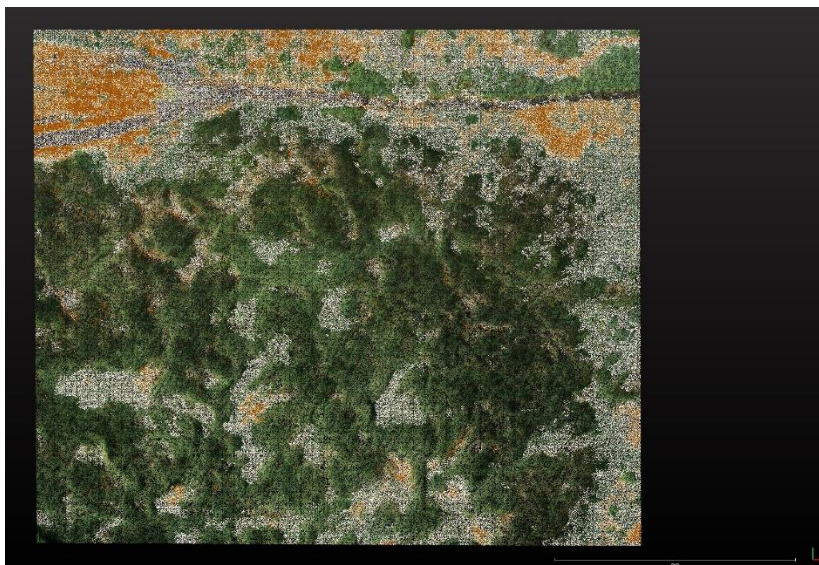


Figure 5-14: Top view of RGB coloured area (left) and spatial distribution (right). Ground points of LiDAR (brown) and photogrammetry (white) point clouds. Scale bar in meters.

A distinct type of vegetation is the flattened reed which grows in patches of disorderly growing stems, possibly enabling both LiDAR and photogrammetry to measure the ground level better than the at the densely tall reed. The ground points show a limited though quite even spaced distribution of LiDAR (brown) points (middle panel) and patches of photogrammetry (white) points. The latter not seldomly coinciding with the vegetation sides of the flattened reed (bottom panel). Statistical analysis show that the mean elevation difference between LiDAR and photogrammetry ground points is in the order of 60 cm for this type of vegetated area.



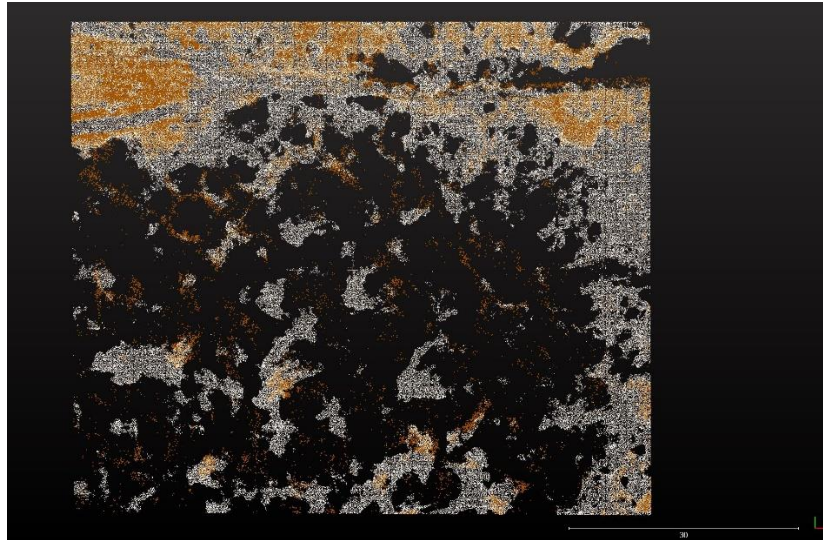
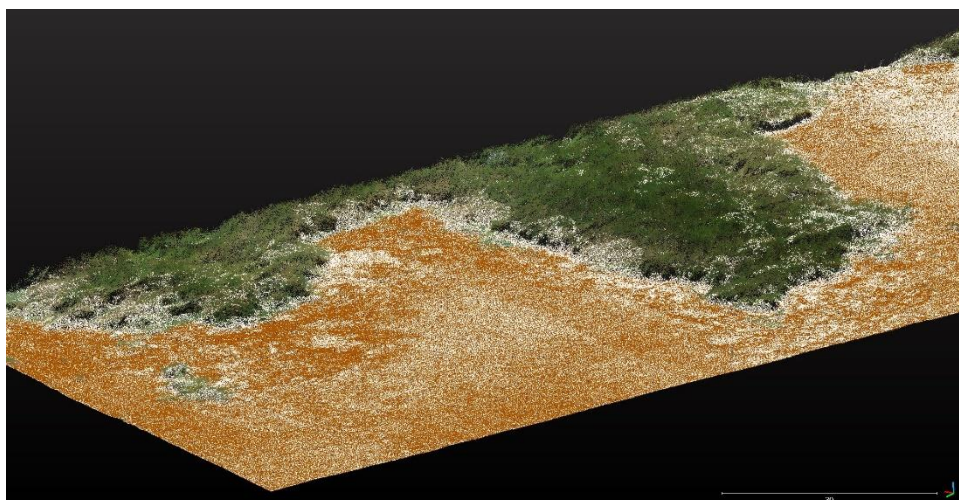
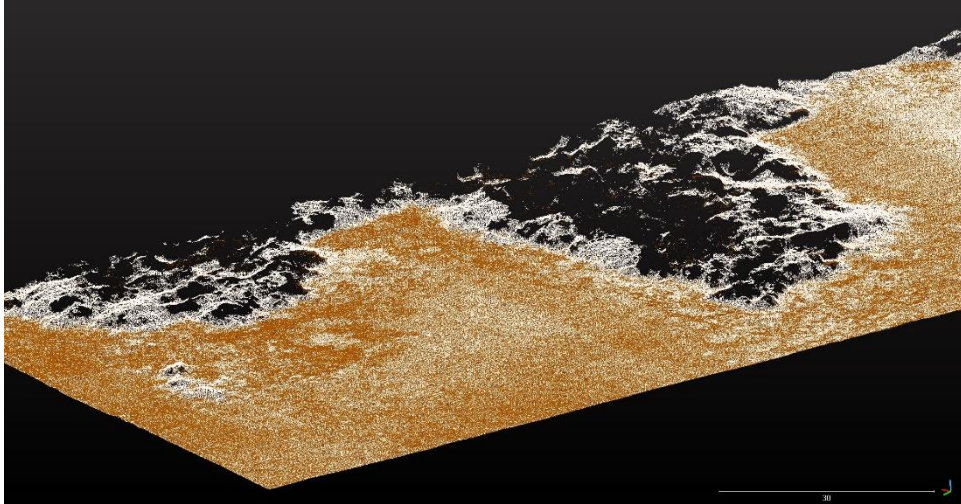


Figure 5-15: Top view of RGB coloured area (top), spatial distribution (middle) of and correctness (bottom) of ground points of LiDAR (brown) and photogrammetry (white) point clouds. Scale bar in meters.

The **Jangwani playground** results are quite representative of the semi cultivated areas south of Morogoro Road. Results of the point cloud assessment (Figure 5-16) show good similarities between LiDAR and photogrammetry on the bare ground and short grass. However, when moving into the taller grass, reed and bush it is only the LiDAR that penetrates the vegetation. Ground points are quite adequately filtered out as non-ground, resulting in no points at these bushes. Like the single bushes next to bar ground, the sides of the vegetation remain in the ground points of the photogrammetry point cloud. LiDAR results show this to a lesser extent, and ground points are measured within the vegetation, be it only a few (bottom).





*Figure 5-16: Oblique view of RGB coloured area (top), spatial distribution (middle) of and side view of correctness (bottom) of ground points of LiDAR (brown) and photogrammetry (white) point clouds. Scale bar in meters.*

The valley near Kawawa road, just south of Hanna Nassif is characterised by very dense, medium tall grass and reed vegetation (Type 3, Figure 5-17). The oblique view of these point clouds show bad results for the photogrammetry point cloud (white) forming a blanket of ground points on top of the vegetation also obscuring the LiDAR ground points (brown, Figure 5-17).

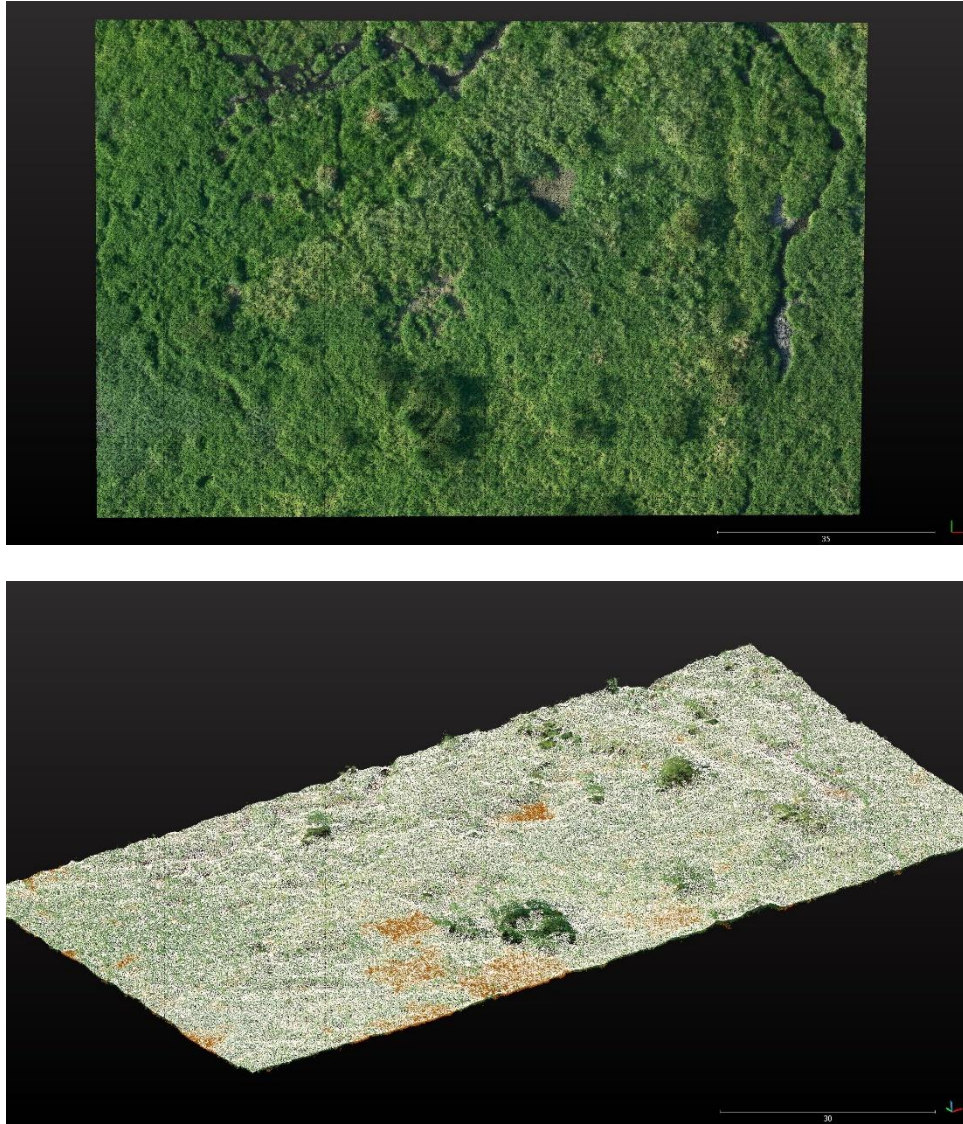
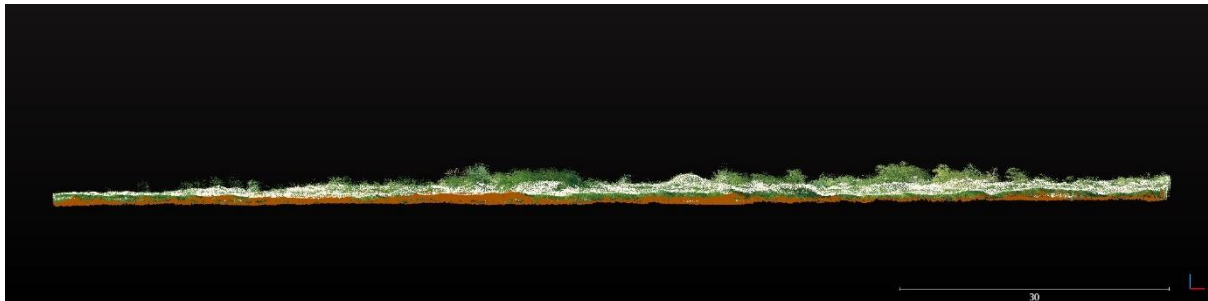


Figure 5-17: Top view of RGB coloured area (top). Oblique view of RGB coloured area and ground points of LiDAR (brown) and photogrammetry (white) point clouds. Scale bar in meters.

The top view of the LiDAR ground points of this area shows quite reasonably spaced ground points, with high concentrations on the low grass. The side view shows a systematic overestimation of the ground points by photogrammetry in the order of 60cm.



*Figure 5-18: Top view of spatial distribution of LiDAR ground points (top) and side view of RGB coloured area and ground points of LiDAR (brown) and photogrammetry (white) point clouds. Scale bar in meters.*

Finally, the point clouds of the urbanised areas were assessed (Figure 5-19). Both techniques perform equally well. At the sides of buildings and houses photogrammetry overestimates the ground level due to the inability to reconstruct the sharp corners of the wall and ground. This photogrammetry point cloud was constructed with images at very low altitude (max 50m) with overlap of 80% forward and 60% sideways and a state of the art RTK-GNSS and INS system for positioning of the images. The vertical accuracy of other photogrammetry sources (fixed wings from high altitudes with less accurate positioning sensors and/or incorporation of ground control points over the area) is not directly comparable with these results. Though in essence the same principles hold.

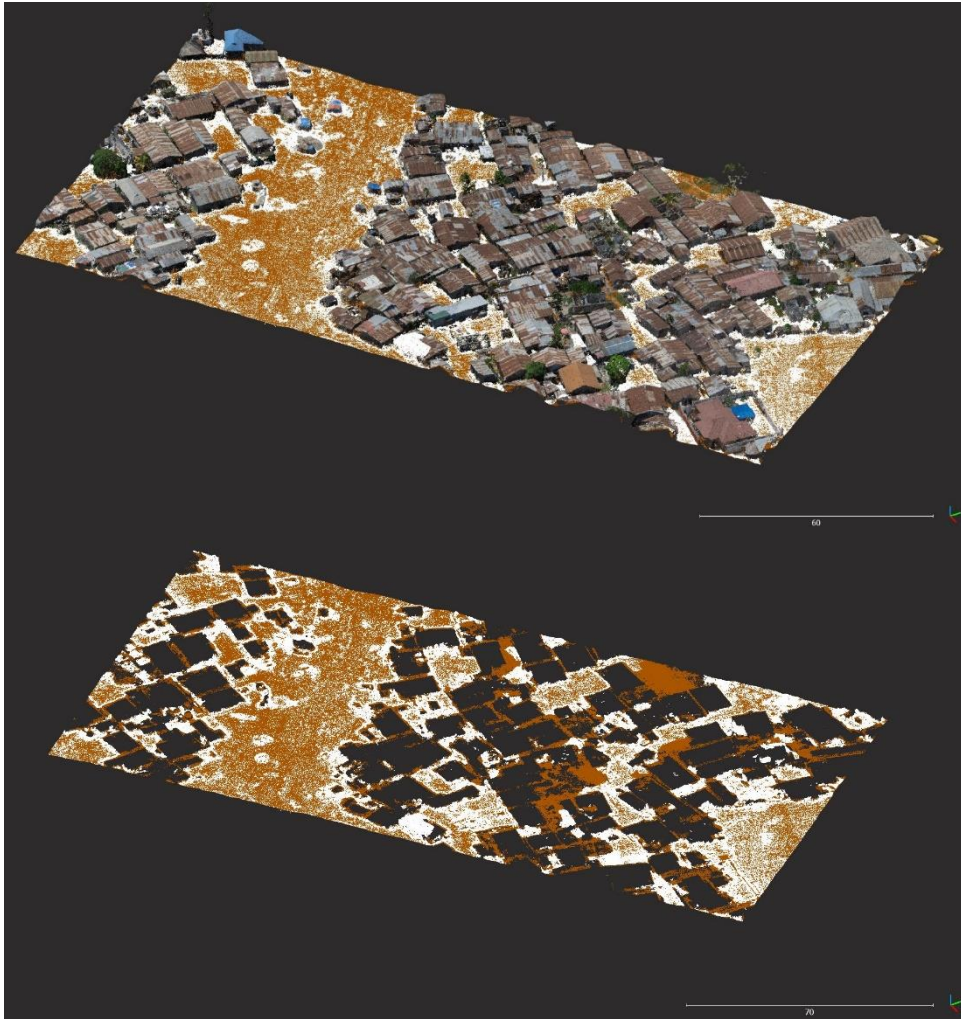


Figure 5-19: Oblique view of RGB coloured area (top) and spatial distribution of LiDAR ground points (brown) photogrammetry (white) point clouds (bottom). Scale bar in meters.

The visual assessment of all point clouds is represented into a table with scores for all terrain types for:

- Correctness of ground point classification
- Spatial distribution of actual ground points

The performance is rated 1 for poor performance, 2 for fair performance and 3 for good performance. Scoring is based on qualitative, visual and manual inspection of the point clouds and figures as presented above and in the appendices.

Table 5-1: Scoring visual interpretation per terrain type, for LiDAR and Photogrammetry

<b>ID</b>	<b>Terrain Type</b>	<b>Accuracy ground points LiDAR (1 - 3)</b>	<b>Accuracy ground points Photogrammetry (1 - 3)</b>	<b>Spatial distribution of actual ground points LiDAR (1 - 3)</b>	<b>Spatial distribution of actual ground points Photogrammetry (1 - 3)</b>
1	Separated dense bushes alternated with low vegetation	3	1	3	1
2	Crops, trees and agricultural grounds	3	3	3	2
3	Dense, medium tall vegetation	3	1	3	1
4	Single bush and dwelling with bare ground	3	2	3	3
5	Jangwani playing grounds	3	3	3	2
6	Bush, short grass with bare ground	2	2	3	2
7	Mangroves with dense canopies	3	1	3	1
8	Mangroves with visible ground level through the (less dense) canopies	3	1	2	1
9	Flattened reed vegetation	3	1	3	1
10	Silvery green dense vegetation	2	1	3	1
11	Single tree, single bush, dense silvery green vegetation	3	2	2	1
12	Trees with dense canopies	3	1	3	1
13	Variety of dense vegetation near swampy terrain	3	1	2	1
14	Long reed, not dense	3	1	2	1
15	Bus depot	3	3	3	3
16	Morogoro road and bus stop	3	3	3	3
17	Urban area	3	3	3	3

## 5.2 Results of statistical analysis

Statistical parameters have been calculated for the LiDAR and photogrammetry ground point clouds for all assessed areas. The most relevant results and insights are discussed below in relation to the presented point cloud assessment in section 5.1.

Table 5-2: Average measured terrain levels (Z) for LiDAR and Photogrammetry. Units in meters unless noted differently

ID	Terrain Type	Area (m <sup>2</sup> )	Z level Average LiDAR	Z level Average Photogrammetry	Delta Z level Average (Photogrammetry - LiDAR)
1	Separated dense bushes alternated with low vegetation	6,052	-24.93	-23.99	0.94
2	Crops, trees and agricultural grounds	10,633	-19.46	-19.37	0.09
3	Dense, medium tall vegetation	9,841	-21.79	-21.21	0.58
4	Single bush and dwelling with bare ground	257	-22.68	-22.32	0.37
5	Jangwani playing grounds	25,407	-22.95	-22.74	0.21
6	Bush, short grass with bare ground	42,789	-22.71	-22.53	0.18
7	Mangroves with dense canopies	7,287	-26.11	-25.25	0.86
8	Mangroves with visible ground level through the (less dense) canopies	15,644	-25.62	-25.34	0.28
9	Flattened reed vegetation	4,843	-22.17	-21.57	0.60
10	Silvery green dense vegetation	7,084	-23.44	-21.18	2.27
11	Single tree, single bush, dense silvery green vegetation	1,469	-22.78	-22.55	0.22
12	Trees with dense canopies	2,083	-25.17	-17.55	7.61
13	Variety of dense vegetation near swampy terrain	10,461	-22.52	-21.46	1.06
14	Long reed, not dense	1,288	-23.04	-20.12	2.93
15	Bus depot	9,933	-21.77	-21.72	0.04
16	Morogoro road and bus stop	3,929	-21.46	-21.38	0.08
17	Urban area	22,734	-21.10	-21.02	0.08

With reference to Table 5-2, the most remarkable results for *the measured terrain levels* are:

- For all terrain types Photogrammetry shows higher average terrain levels than LiDAR;
- Largest differences are calculated for the terrain types with dense and/or high vegetation; e.g. terrain type 10, 12 and 14;
- For the urban areas with hardly any vegetation and relatively large paved and build up areas, like terrain type 15, 16 and 17, the differences are smallest (less than 10cm).

The presented values in Table 5-2 and corresponding results do not indicate vertical accuracies. Vertical accuracies are addressed in section 5.5 Validation results GNSS, including presentation of over- or underestimation of measured UAV LiDAR and Photogrammetry ground point clouds for some terrain coverages.

Table 5-3: Obtained point densities for LiDAR and Photogrammetry

ID	Terrain Type	Area (m <sup>2</sup> )	Density (pnts/m <sup>2</sup> ) LiDAR	Density (pnts/m <sup>2</sup> ) Photogrammetry
1	Separated dense bushes alternated with low vegetation	6,052	15	72
2	Crops, trees and agricultural grounds	10,633	122	89
3	Dense, medium tall vegetation	9,841	19	116
4	Single bush and dwelling with bare ground	257	62	97
5	Jangwani playing grounds	25,407	123	91
6	Bush, short grass with bare ground	42,789	75	99
7	Mangroves with dense canopies	7,287	4	4
8	Mangroves with visible ground level through the (less dense) canopies	15,644	19	10
9	Flattened reed vegetation	4,843	15	53
10	Silvery green dense vegetation	7,084	1	84
11	Single tree, single bush, dense silvery green vegetation	1,469	106	91
12	Trees with dense canopies	2,083	4	24
13	Variety of dense vegetation near swampy terrain	10,461	33	104
14	Long reed, not dense	1,288	1	26
15	Bus depot	9,933	180	103
16	Morogoro road and bus stop	3,929	119	80
17	Urban area	22,734	77	51

With reference to Table 5-3, the most remarkable results for *the ground point densities* are:

- For LiDAR highest ground point densities are obtained in the terrain types with hardly any vegetation (e.g. terrain type 15, 16 and 17), or less dense vegetation (e.g. terrain type 2 and 5);
- For Photogrammetry the ground point densities are higher than LiDAR for the entire project area (70 points/m<sup>2</sup> with Photogrammetry and 57 points/m<sup>2</sup> with LiDAR);
- For the terrain types with dense or tall vegetation Photogrammetry results in higher point densities than LiDAR (e.g. terrain type 10 and 14).

Assuming the ground control points are accurate, it can be stated that a higher point density contributes to the generation of a more accurate DTM. However, ground point densities do not indicate whether the points are distributed equally, which is an important indicator to capture terrain elevation differences over horizontal distance adequately. Point distribution is only assessed visually and reported in section 5.1

Table 5-4: Standard deviations Z values for LiDAR and Photogrammetry. Units in meters unless noted differently

ID	Terrain Type	Area (m2)	Standard Deviation LiDAR	Standard Deviation Photogrammetry
1	Separated dense bushes alternated with low vegetation	6,052	0.29	0.81
2	Crops, trees and agricultural grounds	10,633	0.37	0.39
3	Dense, medium tall vegetation	9,841	0.37	0.48
4	Single bush and dwelling with bare ground	257	0.19	0.54
5	Jangwani playing grounds	25,407	0.17	0.53
6	Bush, short grass with bare ground	42,789	0.23	0.33
7	Mangroves with dense canopies	7,287	0.14	1.48
8	Mangroves with visible ground level through the (less dense) canopies	15,644	0.15	1.07
9	Flattened reed vegetation	4,843	0.54	0.67
10	Silvery green dense vegetation	7,084	1.01	0.99
11	Single tree, single bush, dense silvery green vegetation	1,469	0.21	0.40
12	Trees with dense canopies	2,083	0.14	2.12
13	Variety of dense vegetation near swampy terrain	10,461	0.26	0.73
14	Long reet, not dense	1,288	0.29	0.75
15	Bus depot	9,933	0.11	0.10
16	Morogoro road and bus stop	3,929	0.24	0.32
17	Urban area	22,734	0.31	0.39

With reference to Table 5-4, the most remarkable results for measured standard deviations of the ground Z values are:

- Only two terrain types (10 and 15) show a slightly higher standard deviation (SD) for LiDAR compared with Photogrammetry. The rest of terrain types show quite higher SDs for Photogrammetry
- Lowest standard deviations are obtained for the terrain types with the least vegetation and the largest paved and built up areas (e.g. terrain types 15, 16 and 17)

Standard deviation of measured terrain levels is not a direct indication of accuracy. Large standard deviations of terrain elevation values in a certain area can be caused by i) actual large terrain elevation variation over certain distances (assuming the measurement are accurate), or can be caused by ii) inaccurate measurements representing non-ground objects or incorrect/erroneous measurements. The latter can occur in terrains in which the actual topography has a relatively small terrain elevation variation, like the floodplains of the Lower Basin of the Msimbazi. The numbers presented in Table 5-4 should be interpreted in that context, which makes it plausible that a larger standard deviation of the ground point cloud in this case shows a less adequate representation of continuous terrain elevation.

### 5.3 Resulting UAV Photogrammetry and LiDAR DTMs

The resulting DTMs derived from photogrammetry and LiDAR ground point clouds were made with several grid resolutions:

- 0.25 x 0.25 m
- 0.50 x 0.50 m
- 1.0 x 1.0 m
- 2.0 x 2.0 m

All DTMs and elevation difference maps can be found in Appendix II. No interpolation between points and grid cells was performed. The elevation value of each grid cell is the mean all points within that grid cell. High resolutions (0.25 x 0.25 m) therefore show quite some empty cells (cells with no data). The lower resolution DTMs show fewer empty cells, since a larger area per grid cell is assigned the mean elevation of all points within that grid cell.

Lower resolution grids (larger cell sizes) average out variability in ground level. This is one of the reasons why a uniform resolution of ground points and a high point count, is desirable for accurate DTM generation. The resulting LiDAR DTMs, photogrammetry DTMs and the elevation difference between cells with elevation data are presented in Figure 5-20. Note, cells with no data also render no data when subtracted from cells with data, leaving blank spots on the map.

At first sight the LiDAR DTM shows poorer spatial resolution (Figure 5-20 - top) than the photogrammetry DTM ( - middle). However, the assessment and statistical analysis of the performance to actually measure the ground points, showed that the majority of the vegetated terrain types were not correctly measured by photogrammetry. And in fact, the vegetation tops are now mapped as DTM. This is especially the case in the areas north of Morogoro Road and south of the mangroves. The difference map of both DTMs illustrate this as well (Figure 5-20 - bottom).

The 2.0 m resolution DTMs generated based on the ground points, show a better spatial resolution of the DTM coverage for both LiDAR and photogrammetry (Figure 5-21). However, the non-uniform spatial distribution of photogrammetry ground points in the dense tree and mangroves area, results in less data coverage in that area. Together with the erroneous measurements of the ground points in this area, the photogrammetry DTM should not be used for modelling. This is further confirmed by the difference map of the 2.0 m resolution DTMs (Figure 5-21) showing elevation differences up to 8m in that area.

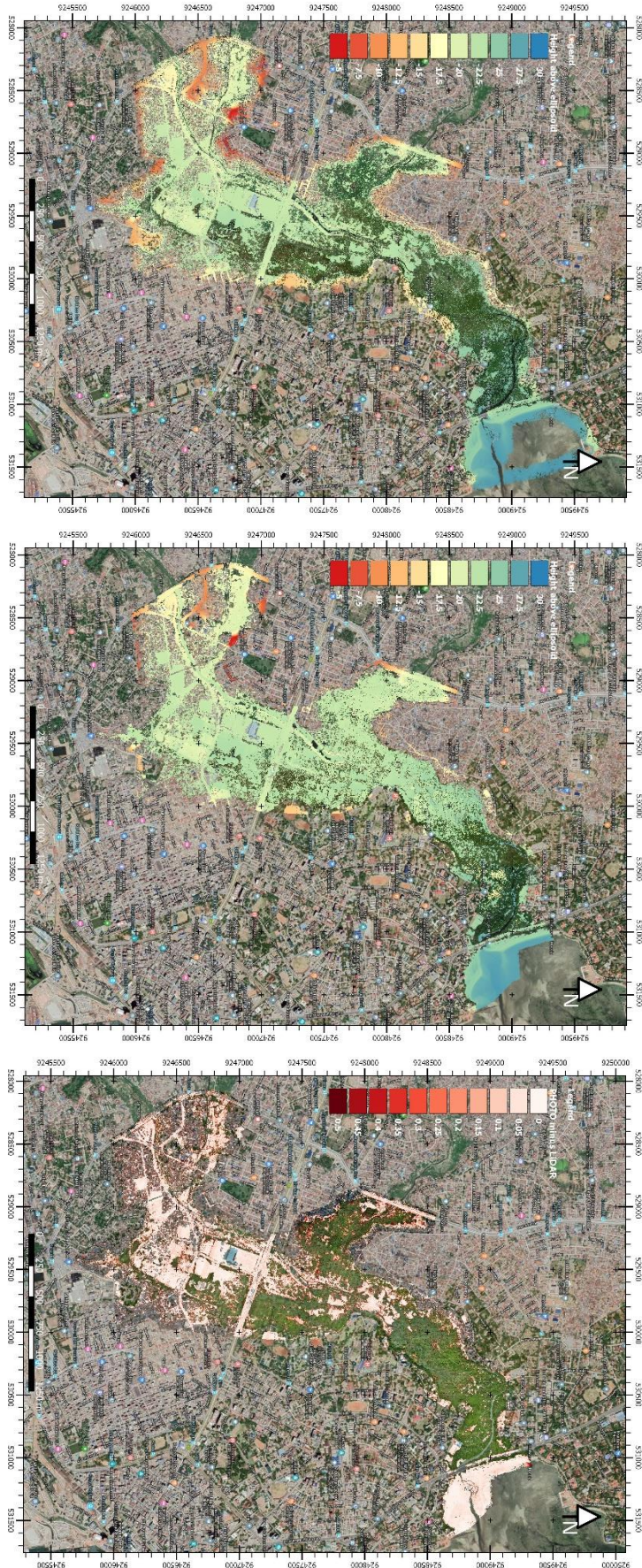


Figure 5-20: 0.25 m resolution DTMs of Lidar (top), photogrammetry (middle) and elevation difference (bottom). Note scale of elevation differences in the figure in (m)

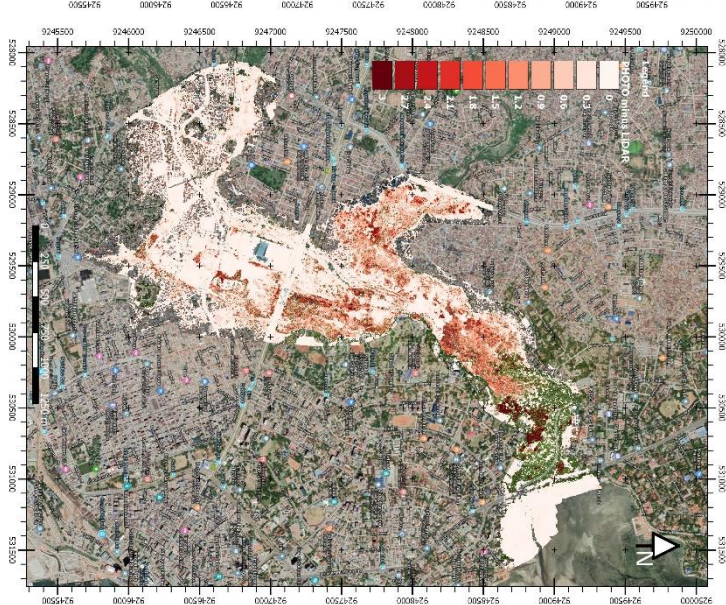
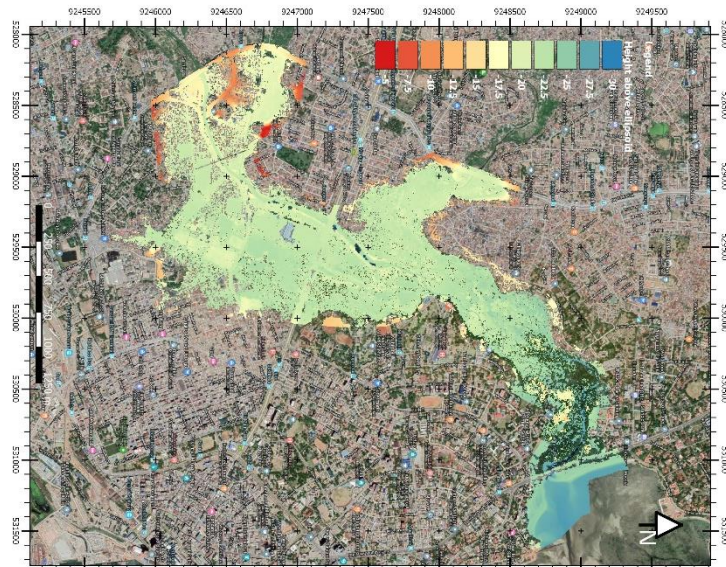
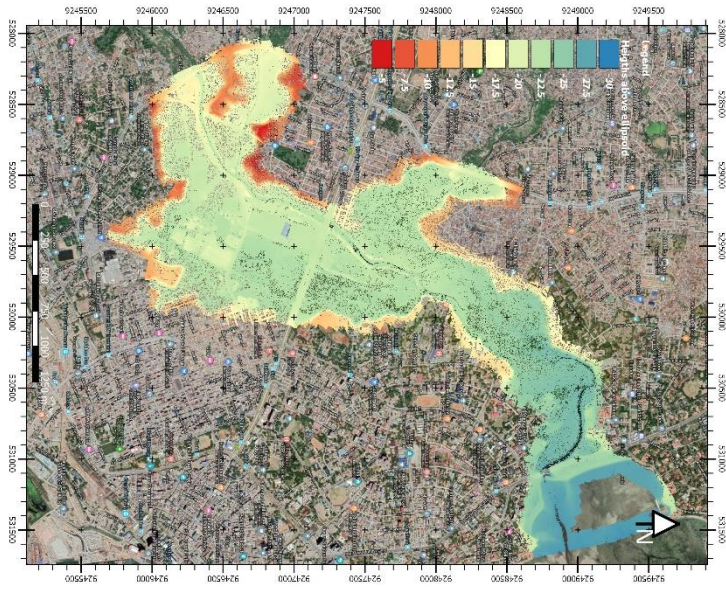


Figure 5-21: 2.0 m resolution DTMs of Lidar (top), photogrammetry (middle) and elevation difference (bottom). Note scale of elevation differences in the figure in (m)

### 5.4 Correlation with land use Msimbazi Basin

Aggregation by manual interpretation of the assessed 17 terrain type areas resulted in 8 larger representative vegetated areas and an urban area covering the entire vegetated area of the Msimbazi Basin (Figure 5-22). Vegetation height and density form the basis for the aggregation, since these proved to be key parameters in the performance to measure the ground.

Urbanised areas were aggregated into a single area. The observations from the performance of both techniques to measure the ground level, statistical analysis and differences in the resulting DTM's were combined to derive generic results for the aggregated areas (Table 5-5).

The results are coupled to the percentage of area covered by these classes in relation to the total vegetated area of the basin, and the ratio of the sum of the vegetated areas and urbanised area with respect to the total basin area.

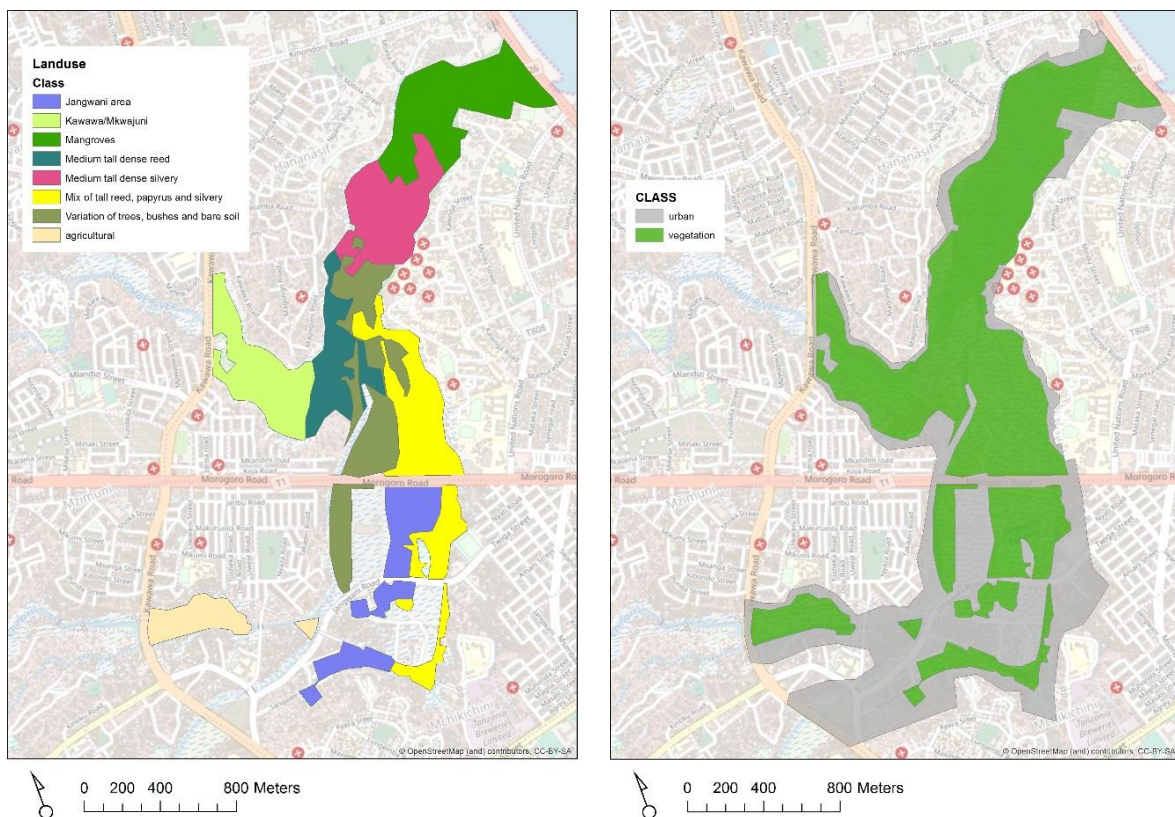


Figure 5-22: Aggregated vegetated areas (left) and the summed vegetated areas and urbanised area (right) of Msimbazi Basin.

These maps and table show that the largest elevation errors in ground level are found in the mangroves & trees area (AA. 4) of which the area forms 17% of the vegetated area in the basin. The location at the outfall of the basin makes it a very important area since it is detrimental for the basin scale gradient in bottom level elevation, greatly determining the water flow.

Table 5-5: Statistics for aggregated vegetated and urban areas in the Msimbazi Basin for LiDAR and photogrammetry ground point measurements.

ID	Aggregated vegetated areas	D Z_Mean	Std_Dev LiDAR	Std_Dev Photogrammetry	Area (m2)	% of Vegetated Basin	% total Basin
AA.1	agricultural	0.16	0.70	0.77	93,360	5%	3%
AA.2	Jangwani area	0.07	0.43	0.52	176,580	10%	6%
AA.3	Kawawa/Mkwajuni	0.57	0.76	0.68	196,274	12%	6%
AA.4	Mangroves	2.94	0.69	3.70	294,880	17%	10%
AA.5	Medium tall dense silvery	1.18	0.97	1.14	214,664	13%	7%
AA.6	Medium tall dense reed	0.64	0.62	0.80	146,050	9%	5%
AA.7	Mix of tall reed, papyrus and silvery	0.57	0.59	0.77	310,001	18%	10%
AA.8	Variation of trees, bushes and bare soil	0.26	0.87	0.95	272,141	16%	9%
					<b>1,703,950</b>	<b>100%</b>	<b>56%</b>
							subtotal

ID	Aggregated urbanised area	D Z_Mean	Std_Dev LiDAR	Std_Dev Photogrammetry	Area (m2)	% of Urbanised Basin	% total Basin
AA.9	Urban	-0.01	2.00	1.83	1,317,899	100%	44%
					<b>1,317,899</b>	<b>100%</b>	<b>44%</b>
							subtotal
					<b>3,021,849</b>		<b>100%</b>
							grand total

The mix of tall reed, papyrus and silvery area (AA. 7), accounting for 18% of the vegetated area also shows considerable elevation differences for the ground levels between the two methods (0.57 m), spanning a large part of the eastern part of the basin.

Areas AA.3, AA.5 and AA.6, show similar elevation differences and form a large part of the central part of the basin, adding up to approximately 33% of the total vegetated basin.

Areas AA.1, AA.2 and AA.8, agricultural, semi cultivated (like Jangwani playing grounds) and bare soil with single trees and bushes show approximate elevation errors of m. These areas represent approximately 30% of the vegetated basin.

### 5.5 Validation results GNSS

The LiDAR DTM was validated against GNSS measurement at Jangwani playing grounds, where bare ground, long reed, short and long grass are present. Results in the long grass show errors in the order of 25 cm. Long reed shows better results with elevation difference between GNSS and LiDAR DTM of 5 to 10 cm. Short grass and bare ground are both showing good results.

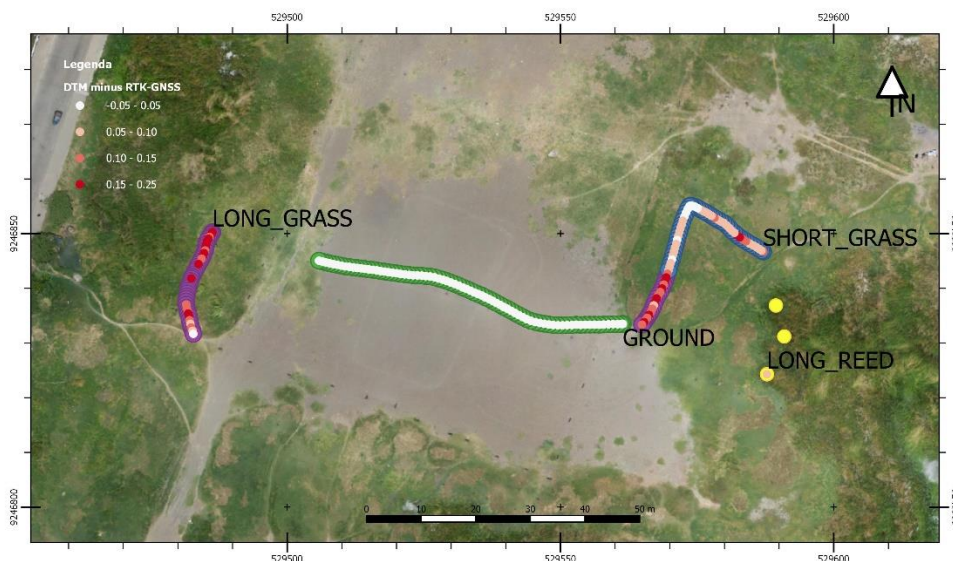


Figure 5-23: LiDAR DTM validation results at Jangwani playing grounds.

The photogrammetry DTM was also sampled on the same locations. The results are presented against the LiDAR DTM validation in a bar plot, indicating a better performance of the LiDAR to measure the ground level for long reed vegetated areas. The other validated vegetation types and the bare ground renders similar performance for both techniques.

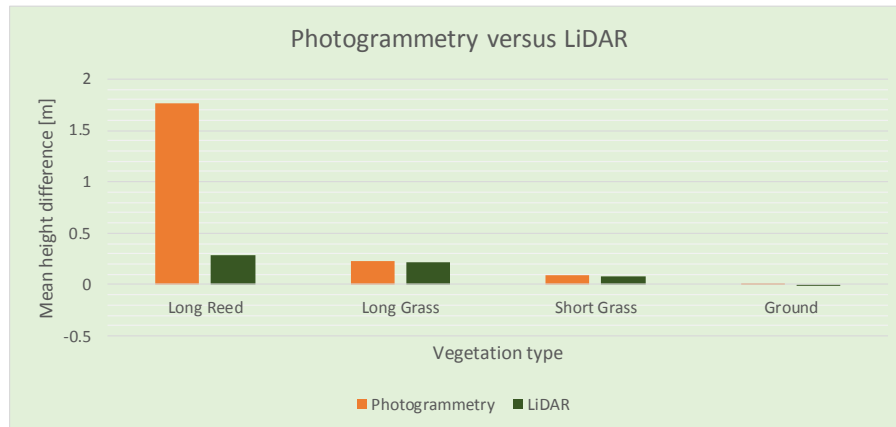


Figure 5-24: Elevation differences of LiDAR and photogrammetry DTM with GNSS measurements of the ground level.

## 5.6 Main Observations

LiDAR performs better in measuring the ground level elevation in vegetated areas than photogrammetry. The spatial resolution of the resulting ground points is more uniform and accurate, rendering more reliable DTMs, which is one of the most important input parameters for flood risk modelling.

Dense vegetation canopies, either formed by (large) trees or densely packed tall grass and reed are areas where photogrammetry structurally overestimates the ground level elevation, approximately by the same height as the vegetation. For areas with trees and mangroves this leads to errors between 5 to 10 m for the Msimbazi Basin, covering approx. 33% of the vegetated area of the basin. For the tall reed and grass, errors are in the order of 1-2 m, covering more than 30% of the vegetated area of the basin. Therefore, the use of photogrammetry in these areas should be avoided for generation of DTMs. Correcting for vegetation height with a constant (height)factor related to the estimated height of the vegetation is discouraged in terrain with (natural) height variability, such as Msimbazi Basin. The canopies or vegetation tops height variability is not coupled to the underlying morphological variability, leading to errors in the derived/constructed DTM, introducing uncertainties into the subsequent modelling and assessments.

Urbanized areas render approximately the same results for both compared datasets. These originated from the same state of the art LiDAR system with camera. When using photogrammetry for accurate elevation data in urban areas, one should always use ground control points for final georeferencing of the model.

## 6. IMPACT OF DTMS ON FLOOD MODELLING RESULTS

The previous chapters elaborated on the comparison between the UAV Photogrammetry and UAV LiDAR results, which mainly provides information about the relative, quantitative and statistical deviation of terrain levels and absolute validation comparison with GNSS ground truth data. In this project the obtained terrain elevation data is to be used for flood modelling assessments, and therefore the data should be tested on fitness for that specific purpose.

### 6.1 Comparison of UAV LiDAR DTM 2019 with DTM 2016

The DTM 2016 has been generated based on aerial image photogrammetry methods, hence acquisition was done by a manned plane. The processing of the LiDAR DTM 2019 has been explained in section 3, and the gridded results have been resampled to a 20m resolution grid suitable for the SOBEK hydraulic flood model. Figure 6-1 shows the delta plot voor the LiDAR DTM 2019 and DTM 2016.

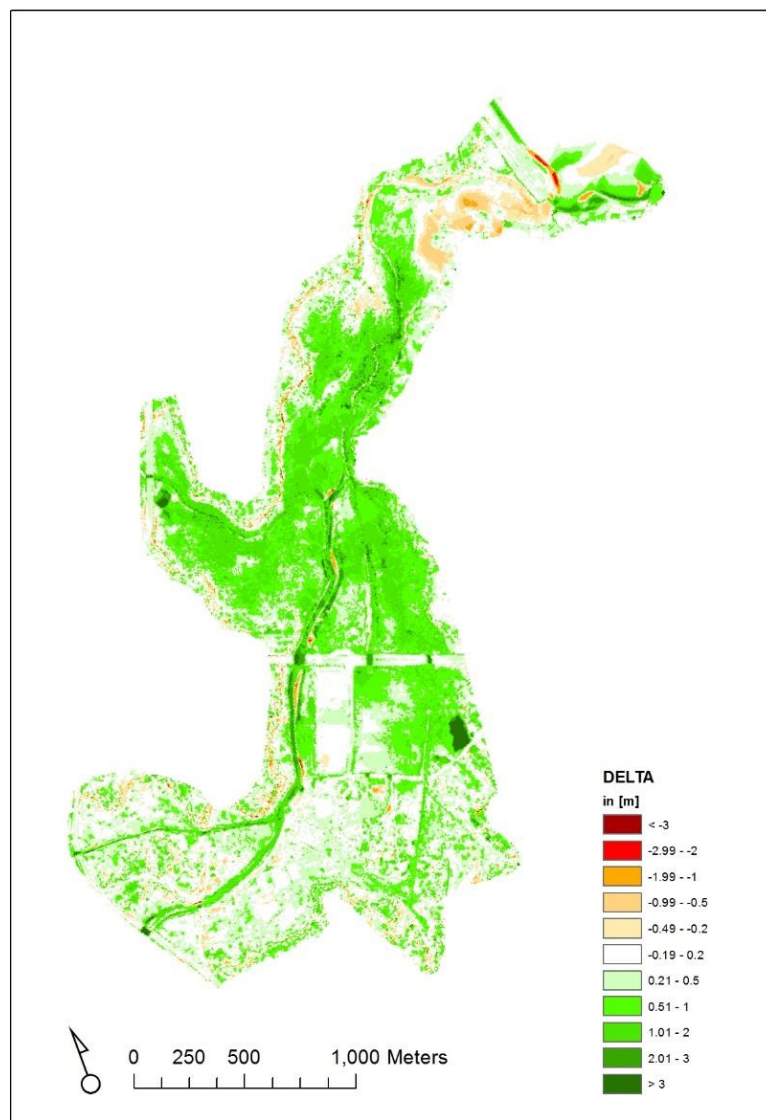


Figure 6-1: Difference between levels of LiDAR DTM and DTM 2016, Green: LiDAR DTM shows higher terrain elevation, Red DTM 2016 shows higher elevation

The following can be observed:

1. It can be clearly seen that the terrain elevation of the LiDAR DTM is for larger parts of the valley higher than the DTM 2016. Responsible for this difference might be the deposition of sediments during flood events that occurred in the two years between the survey campaigns.
2. However, the areas where this is the case, are mainly vegetated. From the comparison results in Chapter 4, it was concluded that photogrammetry cannot measure the ground level in these areas. An explanation for the LiDAR DTM showing higher elevations than the DTM 2016, might also be a result of a too large correction for vegetation height for the DTM 2016. The mangrove area shows erosion between both DTMs in the order of 1-2 m. Most probably this is caused by unreliable bed level elevation in this area in the DTM 2016.
3. Furthermore, the LiDAR DTM shows a ridge along the river. This is reflecting the actual situation along the Msimbazi river, dredging works took place in the past and the dredged material was placed along the river to form an embankment.
4. At the river mouth, outside Selander bridge, there are very high differences between the DTMs, close to the bridge the DTM 2016 shows higher elevations whereas close to the right riverbank the LiDAR DTM resulted in higher levels. These discrepancies can be explained by the very dynamic morphological environment of this area. Coastal processes, as long shore sediment transport and the river dynamic meet at this location causing an ever-changing environment.
5. The LiDAR DTM shows two areas of high elevations in comparison to the DTM 2016 that stand out: The first is at the north-western boundary of the project area, where the Sinza area enters the system. The second one is next to the Jangwani playground. These areas are stockpiles of sand that have been accumulated from dredged sediments of the Msimbazi river after the 2016 survey campaign.
6. It can be observed that main differences of the two survey results are observed in the dynamic environment of the survey area, hence the river and the floodplain. The level of the BRT bus depot and Morogoro Road is consistent. However, along Morogoro road and Jangwani bridge there are three areas where the LiDAR DTM is significantly higher than the DTM 2016. These are the locations of the Box culverts and the Jangwani bridge. The reason for this lies in the incorporation of the bathymetric /terrain level at these location in the DTM 2016. The dimensions of these features were integrated into the model, whereas the LiDAR DTM shows consistently the road deck level of Morogoro Road/Jangwani bridge.

## 6.2 Hydrological and hydrodynamic flood model used

Within the Tanzanian Urban Resilience Program (TURP) Deltares had been assigned to establish and calibrate a flood model that simulates flooding conditions in the lower stretches of the Msimbazi River (ref [5]). A cascaded model, composed of wflow sbm hydrological and SOBEK 1D2D hydraulic model was set up and calibrated. The wflow sbm model was used to assess the catchment area of the Msimbazi river and the river discharges. The 1D2D hydrodynamic SOBEK models river channels in 1D and inundation areas in 2D. The 1D and 2D areas are fully coupled. The 1D part is used to propagate floods in river channels and the 2D component is used to model the inundation of land surface areas in terms of 2D flood propagation. It has been run with observed rainfall from the Trans-African Hydro-Meteorological Observatory (TAHMO) and calibrated based on the flood event in October 2017. More information about this model can be obtained from the Deltares report (ref [5]).

To show the impact of using different DTM's on flood modelling results, a flood simulation with the DTM 2016 incorporated in the flood model is compared with a simulation in which the LiDAR DTM

incorporated. The DTM 2016 was used for most of the preliminary flood mitigation and protection designs, whereas the LiDAR DTM is planned to be used for the detailed studies of the envisaged interventions. For the run with the LiDAR DTM the DTM was updated; the other flood model parameters were kept identical to the run with the DTM 2016. A rainfall event with a 10 year return period was used for both runs. By only changing the DTM parameter the impact of this main input to the flood model results can be assessed most purely. The results were compared for several model outputs, viz. development of flow velocities, flood depth and flood levels.

### 6.3 Flood Modelling Results

Figure 6-2 shows the difference between the maximum flood levels of the LiDAR DTM and the DTM 2016 simulation.

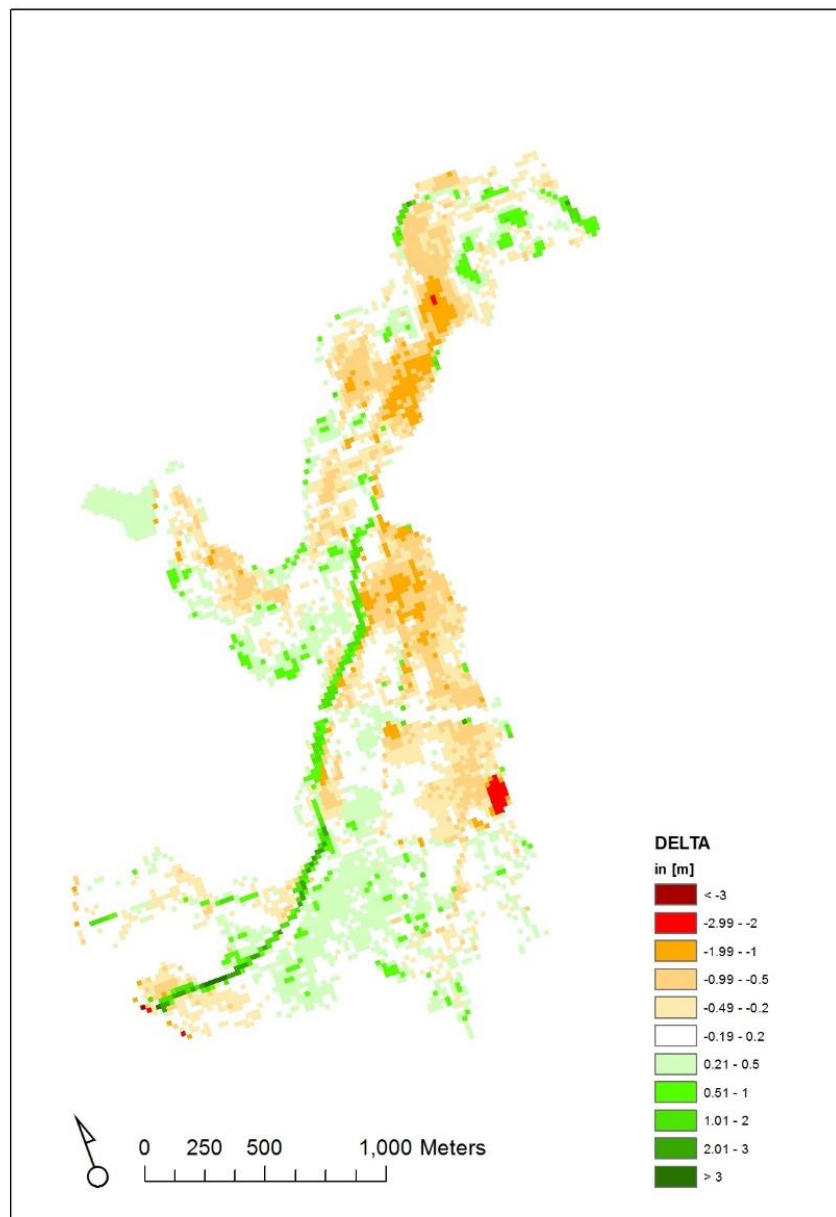


Figure 6-2: Difference between maximum flood depths of LiDAR DTM and DTM 2016, Green: LiDAR DTM shows larger flood depth, Red: DTM 2016 shows larger flood depth

Overall, the maximum flood depth seems less for the model runs performed based on the LiDAR DTM than the ones performed with the DTM 2016. This is true mainly for the area around the Jangwani

playground and the upper part of the Msimbazi River. Regarding the hydraulic process of flooding, this can be based on the differences in the levels of the DTMs. Since the ground level of the LiDAR DTM is in general higher in the floodplain, it is expected that water will spread more over the area, but the water depth will be less. In the River channels however, the water depth based on the LiDAR DTM is higher. Looking in detail at the comparison of the DTMs it can be spotted that the levels of the DTM 2016 in the channels itself is higher in comparison to the LiDAR DTM. Hence, above mentioned explanation fits here as well: Lower levels lead to higher levels but to a more concentrated area

The flooding event modelled is covering a time span of 72h. development of the flood over time based on the two modelling can be observed in 4h timesteps in Appendix IV. Looking at those images it becomes evident, that the flood modelled based on the LiDAR DTM is in its expansion phase (first 24 hours) highly focused around Morogoro Road. In comparison to that the flood modelled based on the DTM 2016 is also developing in the lower Msimbazi river and the Sinza river.

After 36 hours the flood based on the LiDAR DTM shows a greater water depth South of Morogoro Road whereas the north of the road similar flood depths is reached. After 60 hours the peak of both flood models has developed. Left of the Jangwani playground, where the BRT bus depot is located, a greater flood depth can be observed in the LiDAR based flood model. However, in the area of the Mangroves, the great flood depth is bigger in the DTM 2016 based model. During the declining phase of the modelled flood event, it can be observed that the bigger water depths vanish faster in the model based on the LiDAR DTM.

A more detailed analysis that shows the influence of the different DTM more clearly can be made when comparing the resulting Hydrographs in specific locations. Overall seven of those locations were chosen for this task (see Figure 6-3). In the following, the locations 3, 4, 5 and 6 are analysed in detail. All hydrographs with a brief analysis are in Appendix IV.

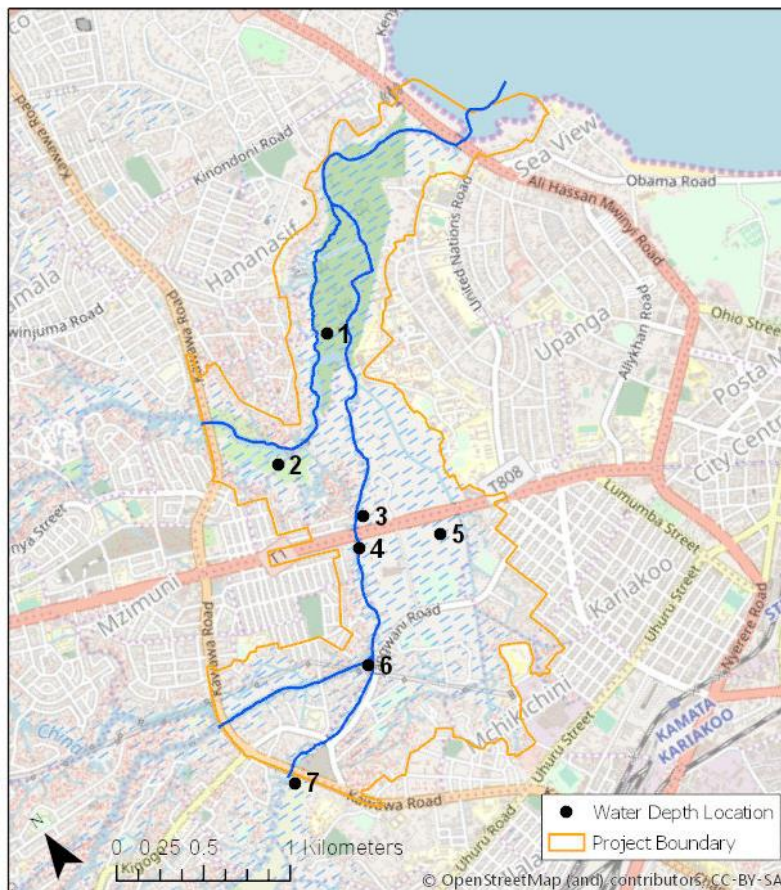
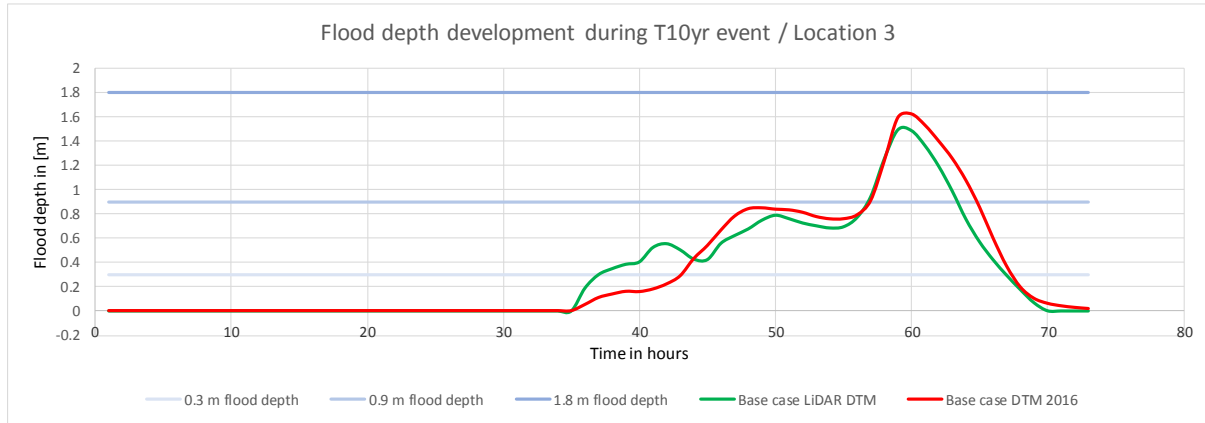
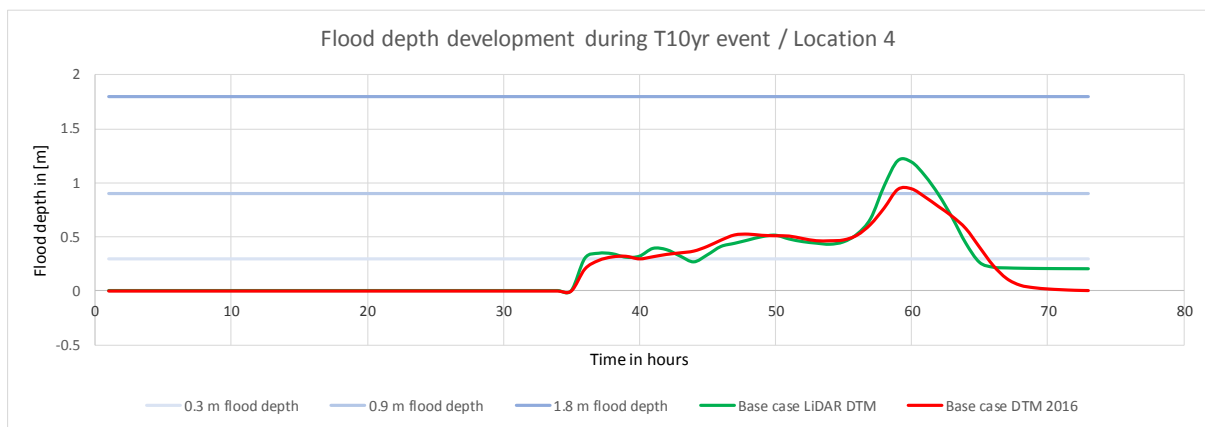


Figure 6-3: Locations of water depth measurements

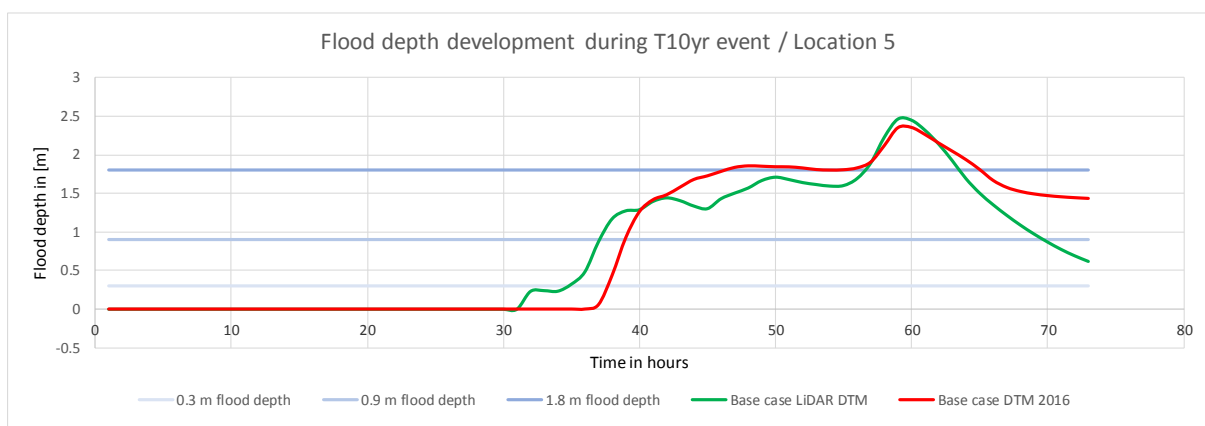
Location 3 is north of Jangwani Bridge, downstream the Msimbazi River. Comparing the hydrographs based on the two different flood models, it can be stated that the one based on the LiDAR DTM shows a slightly shorter inundation period. Also, a greater flood depth during the first 10 hours (35-45 h on the x-axes) of the flood event. After this period, the maximum flood depth based on the DTM 2016 is larger.



Location 4 is downstream Jangwani bridge, next to the bus depot. At this location it can be observed that the duration and timing of the flood event is quite comparable. However, there is quite a significant difference in the peak of the flood (maximum flood depth). The LiDAR DTM based model shows a peak of approximately 1.30 m whereas the DTM 2016 based model reaches a maximum of 90 cm. This is important as it influences design criteria for the critical infrastructure in the area (bridges).



Location 5 are the Jangwani playing grounds. Here you can clearly see that the inundation starts earlier (about 5 to 6 hours) in the LiDAR DTM simulation compared with the DTM 2016 simulation.



Location 6 is at the confluence of the Kibangu and the Msimbazi River. The hydrograph below show that the inundation period for both modelled flood events are almost similar, however the flooding based on the LiDAR DTM starts and finishes earlier. Hence a shift in the time axes of approximately 5 to 6 hours can be observed. Also the two peaks based on the LiDAR DTM are significantly higher than the ones modelled by the DTM 2016 (30 to 40 cm).

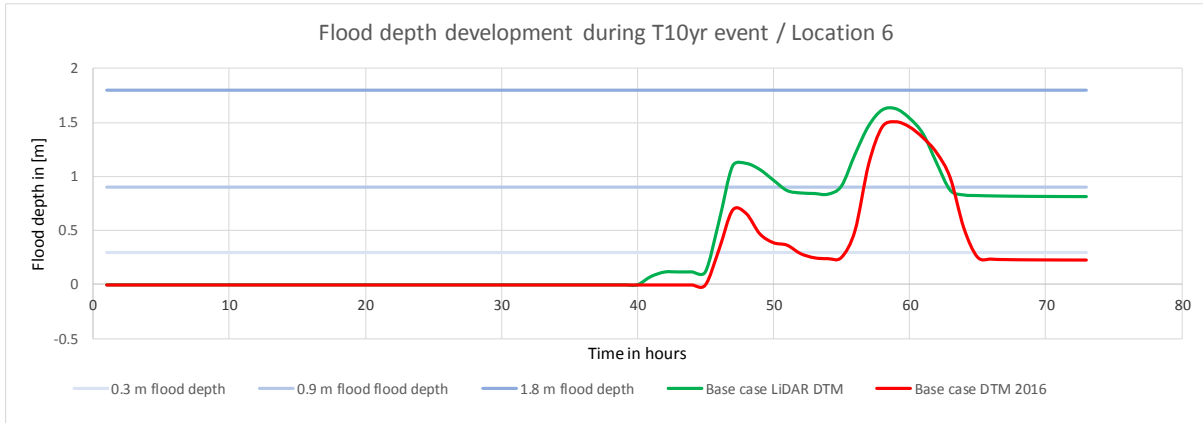


Figure 6-4 shows the difference in the modelled maximum flow velocities between the LiDAR DTM and the DTM 2016.

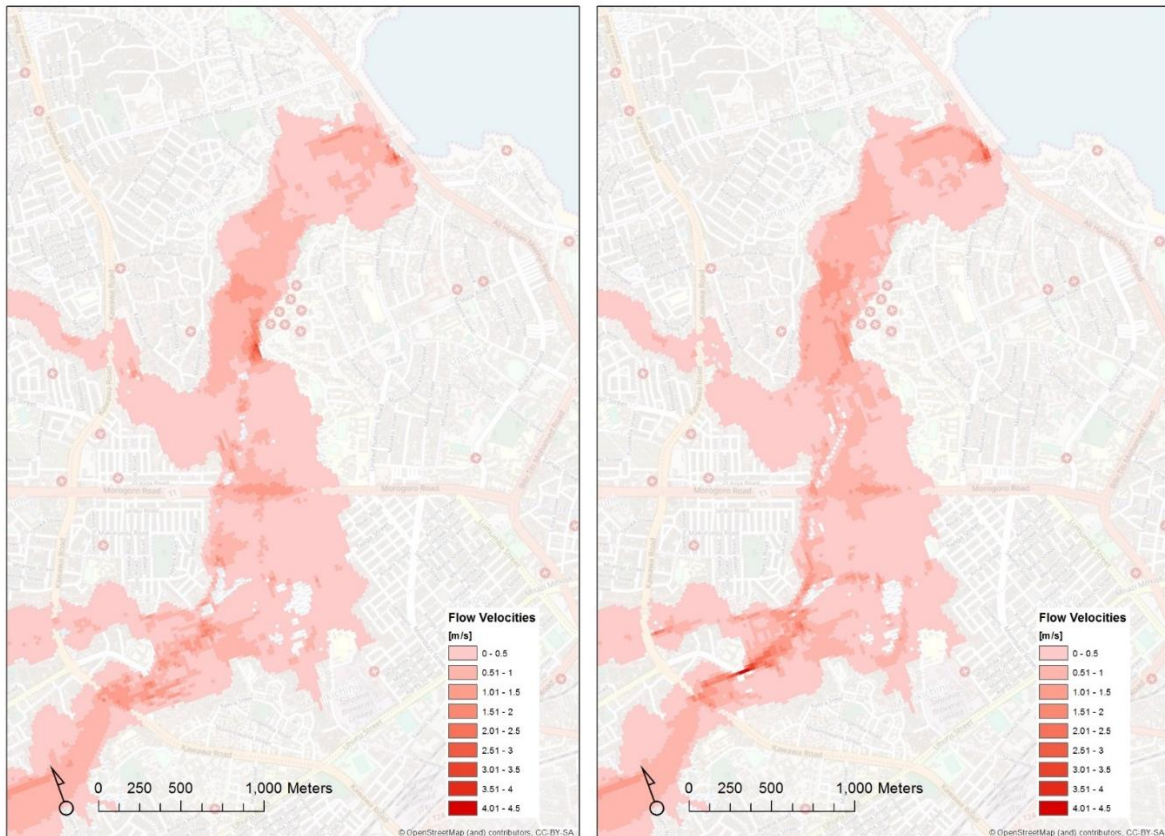


Figure 6-4: Maximum Flood Velocities based on model with DTM 2016 (left) and LiDAR DTM (right)

In general the maximum flow velocities reached are quite comparable, as indicated in Figure 6-4. In the Jangwani valley both models show similar results. However, there are two observations of differences to be made:

- Maximum flow velocities reached around Muhubili hospital, at the eastern part of the model, north of Jangwani playground are significantly higher in the flood model based on the DTM 2016
- Maximum flow velocities reached in the Kibangu and Msimbazi River before entering the Jangwani valley are much higher in the flood model based on the LiDAR DTM

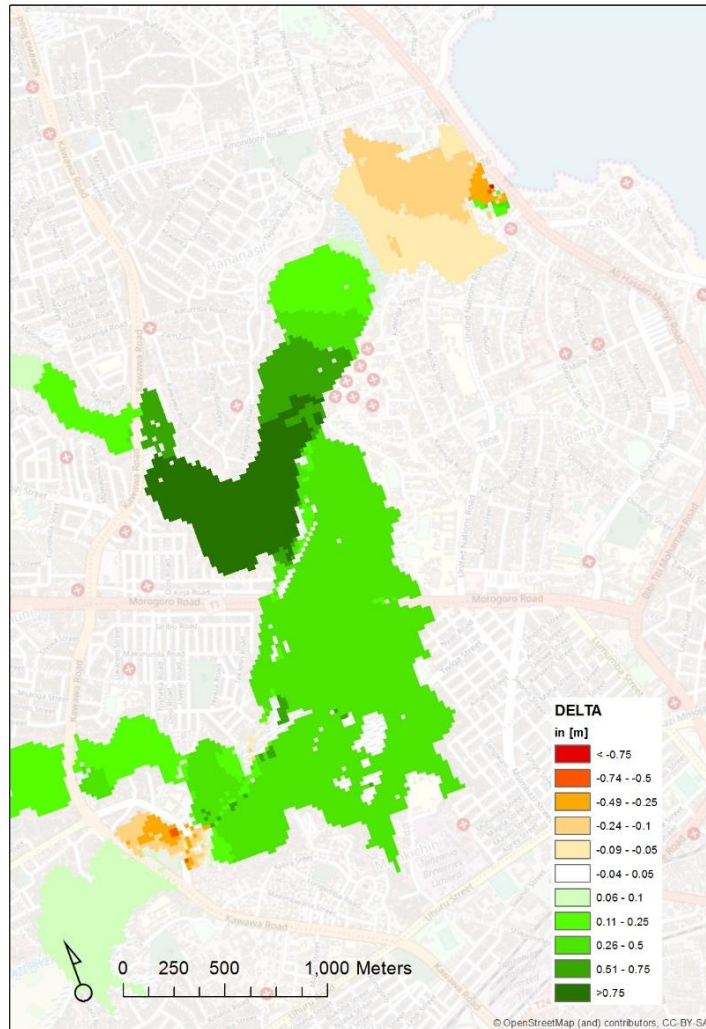


Figure 6-5: Maximum Flood Level Comparison, Green: LiDAR DTM shows larger flood levels, Red: DTM 2016 shows larger flood levels

Comparing the different maximum flood level, it can be observed that for the main assessed area the flood model based on the LiDAR DTM shows a greater flood level, especially in the confluence of the Sinza river flood plain and the Msimbazi river. In the Mangrove area and upstream of the Msimbazi, the DTM 2016 shows greater flood levels.

## 6.4 Interpretation of the Results

From the comparison of the flood modelling results the clearest differences are observed in the flood levels, which are higher for the LiDAR DTM run than the DTM 2016. Also earlier inundation in the Jangwani Valley with the LiDAR DTM results is apparent. Most of these differences can most likely be attributed to sedimentation of the river courses and the floodplains between 2016 and 2019 as well as incorrect vegetation mapping for generation of the DTM 2016. These morphological processes in

higher terrain elevations over time, which can be clearly seen in the delta plot of the two DTMs, and which also leads to higher flood level model results. Attributing differences in the results of the flood modelling results to accurateness and resolution of the two DTMs is very difficult and cannot be proven, among other reasons because the post-processing of the point clouds of both datasets was much different. The LiDAR DTM has been generated almost completely automatically, whereas the DTM 2016 was processed by means of tie lines and local surveys to estimate terrain levels for vegetated area.

## 7. CONCLUSIONS AND RECOMMENDATIONS

### 7.1 Conclusions

This comparison described the principles of photogrammetry and LiDAR, acquisition and postprocessing aspects. The core of the comparison is the assessment of the performance of UAV photogrammetry and UAV LiDAR to measure the ground levels in a Sub-Saharan context, for accurate DTM generation for flood risk modelling.

From an acquisition point of view, UAVs for photogrammetry surveys are cheaper and can survey an area faster than UAV LiDAR. However, the necessity of placing and measuring ground control points should be taken into account for photogrammetry. Ground control points are not necessary for LiDAR surveys, however, measuring some 3D objects by ground GPS RTK measurements within the survey area is advised to validate the planimetric and height accuracy of the point cloud. Photogrammetry surveys are often performed with fixed wing systems, whereas most (affordable) UAV LiDAR systems are based on multi rotor platforms having the implication that a smaller area can be covered with one flight.

Photogrammetry processing involves triangulation of pixels in thousands of images, which can be done semi automatically. Georeferencing by means of marker placement is a time-consuming part of the processing, which can be decreased by making use of an RTK-GNSS drone. The resulting photogrammetry model is however always a reconstruction (not a measurement) of what is visible in the images. Unsharp, poorly lit images, or images lacking contrast will only manifest after survey, in post processing, and result in a poor reconstruction of an area. Furthermore, when the ground level is not visible in the images, it will not be reconstructed either. Photogrammetry renders, by definition, a DSM of an area. A DTM can be obtained by ignoring/rejecting all other points than ground points. Depending on the remaining ground points a DTM can be interpolated based on these points. With photogrammetry the amount of reliable ground points in vegetated areas of the Msimbazi Basin was found limited.

A LiDAR survey is a direct measurement of an area and provides real-time assessment of the quality of the point cloud while the UAV is flying over the area. For the largest part, post processing is performed automatically after finding the correct values for the algorithms on a representative (smaller) subarea. The main advantage of LiDAR is that it can penetrate vegetation resulting in ground points in between and under vegetation. This results in a more uniform distribution of ground points over the measured area.

The assessment of the performance of both techniques to measure the ground level elevation was performed by analysis of 17 sub areas; 14 vegetated areas and 3 urbanised areas. Point clouds were visually assessed on i) density and spatial distribution of ground points over the area, ii) correctness of ground points based on elevation and iii) relative elevation differences. Furthermore, statistics were calculated to quantify the comparison.

LiDAR performs better in measuring the ground level elevation in vegetated areas than photogrammetry. The spatial resolution of the resulting ground points is more uniform and accurate, rendering more reliable DTMs, which is one of the most important input parameters for flood risk modelling. Figure 7-1 is presented to illustrate the above for a dense tree canopy in the basin.

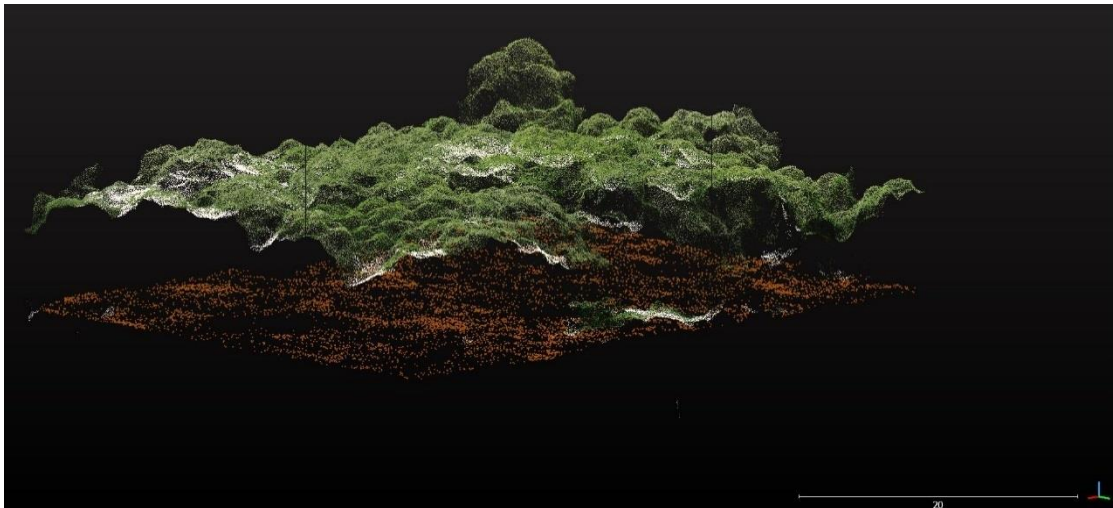


Figure 7-1: Oblique view of the RGB coloured point cloud of the dense tree canopy area. Ground points of LiDAR (brown) and photogrammetry (white) point clouds. Scale bar in meters.

These results of the visual assessment and statistical analysis were aggregated to basin scale by forming 8 representative classes for the vegetated area and one class for the urbanised areas. Percentages of basin coverage of these classes and their main statistics were calculated based on these aggregated areas as indicated in section 5.4 of this report.

Table 7-1: Statistical results of LiDAR and Photogrammetry methods for the aggregated areas

ID	Aggregated vegetated areas	D Z_Mean	Std_Dev LiDAR	Std_Dev Photogrammetry	Area (m2)	% of Vegetated Basin	% total Basin
AA.1	agricultural	0.16	0.70	0.77	93,360	5%	3%
AA.2	Jangwani area	0.07	0.43	0.52	176,580	10%	6%
AA.3	Kawawa/Mkwajuni	0.57	0.76	0.68	196,274	12%	6%
AA.4	Mangroves	2.94	0.69	3.70	294,880	17%	10%
AA.5	Medium tall dense silvery	1.18	0.97	1.14	214,664	13%	7%
AA.6	Medium tall dense reed	0.64	0.62	0.80	146,050	9%	5%
AA.7	Mix of tall reed, papyrus and silvery	0.57	0.59	0.77	310,001	18%	10%
AA.8	Variation of trees, bushes and bare soil	0.26	0.87	0.95	272,141	16%	9%
					<b>1,703,950</b>	<b>100%</b>	<b>56%</b>
							subtotal

ID	Aggregated urbanised area	D Z_Mean	Std_Dev LiDAR	Std_Dev Photogrammetry	Area (m2)	% of Urbanised Basin	% total Basin
AA.9	Urban	-0.01	2.00	1.83	1,317,899	100%	44%
					<b>1,317,899</b>	<b>100%</b>	<b>44%</b>
							subtotal
					<b>3,021,849</b>	<b>100%</b>	grand total

Dense vegetation canopies, either formed by (large) trees or densely packed tall grass and reed are areas where photogrammetry structurally overestimates the ground level elevation, approximately by the same height as the vegetation.

For areas with trees and mangroves this leads to mean errors of approximately 3 m, with maximum errors in DTMs between 5 to 10 m for the Msimbazi Basin, covering approx. 33% of the vegetated area of the basin.

For the tall reed and grass, errors are in the order of 1m, covering more than 30% of the vegetated area of the basin Therefore, the use of photogrammetry in these areas should be avoided for generation of DTMs.

Correcting for vegetation height with a constant (height)factor related to the estimated height of the vegetation is discouraged in terrain with (natural) height variability, such as Msimbazi Basin. The canopies or vegetation tops height variability is not coupled to the underlying morphological

variability, leading to errors in the derived/constructed DTM, introducing uncertainties into the subsequent modelling and assessments.

Urbanized areas render approximately the same results for both compared datasets. These originated from the same state of the art LiDAR system with camera. When using photogrammetry for accurate elevation data in urban areas, one should always use ground control points for final georeferencing of the model.

From the perspective of DTM usage for the purpose of hydrological and hydraulic flood modelling the following can be concluded from the UAV comparative analysis:

- Generally, for vegetated areas the photogrammetry results show a larger overestimation of the terrain levels than the LiDAR results and introduce undesirable uncertainties in the model.
- Urbanised areas or semi cultivated areas with bare ground and scattered vegetation render equally useful results with both techniques.

The assessed and reported impact of using different DTMs on flood modelling results (section 6) is not directly related to the comparison between the UAV photogrammetry and LiDAR results, but rather serves as an indication of how sensitive hydrological, hydrodynamic flood models are to different DTMs. The results in section 6 show it's fairly sensitive, impacting timing and magnitude of flood depth development and particularly flood level development significantly. In case the Msimbazi Lower Basin had not been re-surveyed in Feb 2019 and the hydraulic modelling results with the DTM 2016 would have formed the basis for design, the adaptive and protective measures around Jangwani area (middle part of the Study area) would have been designed about 30-40 cm too low in absolute levels. This is considered a large impact.

## 7.2 Recommendations

- In case it needs to be decided which acquisition method should be adopted to generate a DTM, it is recommended to first assess typical terrain cover. This can be done through obtaining and analysing satellite/ortho-imagery/drone flight images, and subsequently compare identified coverage with the results from this study, in particular as presented in section 5.1 and section 5.2. Based on comparison and possible similarities between the vegetation covers with associated results and recommendations, this will help to inform whether to choose LiDAR or photogrammetry.
- In view of the higher accuracy and fitness for flood modelling purposes, it is recommended to conduct a UAV LiDAR survey in case a project has to deal with the following conditions:
  - o hydraulic modelling needs to be performed;
  - o the basin is covered with vegetation (particularly close to the river course);
  - o hardly any data is available (data poor);
  - o and, a complete baseline dataset is required.

A baseline usually serves as a 0-situation for all type of studies for which the baseline's data is going to be used for. Therefore, the baseline should have an accuracy and resolution as high as possible. Dealing with a 0-situation containing many uncertainties delays projects and results in less suitable solutions to the problems. Moreover, if a 0-situation will be used as ground truth for all subsequent studies (e.g. from risk studies to concept design to detailed design of mitigation interventions) errors will propagate through all project phases. Often this results in conservatively designed and more expensive interventions.

- In line with previous recommendation point it is noted that UAV LiDAR surveys are more expensive than UAV photogrammetry surveys. However, the higher costs for UAV LiDAR will easily pay off in subsequent risk and design studies by avoided uncertainties. Uncertainties usually lead to additional study time and delays, which in turn can be expressed in a cost reduction. Besides this, less uncertainty in baseline data for designs provides a basis for optimisation, hence reduces the need to over-dimension designs to account for the uncertainties resulting in a higher cost-efficiency.
- The Lower Basin of the Msimbazi River is very flood prone. Along with the floods also large loads of silt and sand which have eroded further upstream are being transported with the water flow, and settle in the Lower Basin. Floods and sedimentation are intertwined issues not only present in Dar es Salaam, but occur in many more rapidly growing cities in river basins across the world. River erosion and sedimentation processes result in changing morphological conditions, among other aspects expressed in changing bathymetric river bed levels and changing topographic levels of e.g. levees and floodplains. After the floods the sedimented areas are like bare soils as assessed in section 6. For enhancing the city's resilience to flooding recurrent surveys are required to monitor the behaviour of the river and its morphology. With such a dynamic river using recent, updated and accurate data for the specific assessments is key to advice and act adequately. Based on the results of this comparative analysis it is considered sufficiently accurate to conduct recurrent surveys for aforementioned purpose with UAV Photogrammetry.

If LiDAR is not an option, budget wise, survey teams can be send out into the field with RTK-GNSS equipment to measure the ground level elevation in between the vegetation. Depending on the expected variation in terrain elevation teams can determine an appropriate interval distance for the transects. Fundamental is that within all different patches of vegetation the ground level elevation is measured, in order to correct a photogrammetry DTM for the full coverage of the project area. Having said this, it is an extremely laborious and tedious work of which the final corrections (e.g. by means of additional tie lines) to the DTM need be performed by a (GIS) data and morphology expert. To give an indication; experts that generated the DTM 2016 indicated that it took additional time in the order of weeks to correct the photogrammetrically derived DTM for hydraulic modelling purposes. Also, the ground level within the mangroves will be hard to measure because GNSS reception is limited. Besides this, there could be safety issues in the field.

## 8. REFERENCES

- [1] Msimbazi Opportunity Plan – Transforming the Msimbazi Basin into a Beacon of Urban Resilience – Volume A – Strategy and Management Framework – Jan 2019
- [2] Msimbazi Opportunity Plan – Transforming the Msimbazi Basin into a Beacon of Urban Resilience – Volume B – Detailed Plan of the Lower Basin – Jan 2019
- [3] Shore Monitoring & Research and CDR International; Bathymetric and UAV-LiDAR Topographic Survey of Msimbazi River Area, Tanzania – Field Report – April 2019
- [4] COWI – Flood Mitigation in the Msimbazi Valley – Final Report - 2018
- [5] Deltares – Development of a Hydrological and Hydrodynamical Model of the Msimbazi basin – July 2018

## APPENDIX I - APPENDIX PERFORMANCE MEASUREMENT GROUND POINT

## APPENDIX II - DTMS

## APPENDIX 3 - DTM 2016 COMPARISON

## APPENDIX IV - COMPARISON MODELLING RESULTS